МІНІСТЕРСТВО ОСВІТИ І НАУКИ УКРАЇНИ

Національний університет «Запорізька політехніка»

Електротехнічний факультет
(повне найменування факультету)

Електричні та електронні апарати
(повне найменування кафедри)

Пояснювальна записка

до магістерської роботи
магістр
(ступінь вищої освіти)

на тему Дослідження та розробка електромагнітного приводу контактора змінного струму, 380 В, 110 А
(назва теми)

Виконав(ла): студент(ка) II курсу, групи Е-413ам

Спеціальності 141 Електроенергетика,
(код і найменування спеціальності)
електротехніка та електромеханіка

Освітня програма (спеціалізація)
Електричні та електронні апарати

НЕВТИРЯ К.С.
(ПРІЗВИЩЕ та ініціали)

Керівник БЛИЗНЯКОВ О.В.
(ПРІЗВИЩЕ та ініціали)
Рецензент САХНО О.А.

2024

МІНІСТЕРСТВО ОСВІТИ І НАУКИ УКРАЇНИ

Національний університет «Запорізька політехніка»

Факультет Електротехнічний факультет
Кафедра „ Електричні та електронні апарати ”
Спеціальність 141 Електроенергетика, електротехніка та електромеханіка
(назва освітньої програми (спеціалізації)

ЗАТВЕРДЖУЮ
Завідувач кафедри проф. АНДРІЄНКО П.Д.
_____
«_____» _____ 20___року

З А В Д А Н Н Я

НА МАГІСТЕРСЬКИЙ ПРОЄКТ (РОБОТУ) СТУДЕНТА(КИ)

НЕВТИРЯ Кирило Сергійович
(ПРІЗВИЩЕ, ім’я, по батькові)

1. Тема роботи: Дослідження та розробка електромагнітного приводу контактора змінного струму 380 В, 110 А.

керівник роботи: к.т.н., доц. БЛИЗНЯКОВ Олександр Вікторович
(науковий ступінь, вчене звання, ПРІЗВИЩЕ, ім’я, по батькові)

затверджені наказом закладу вищої освіти від «_20_» _листопада_ 2024 року № 481

2. Строк подання студентом роботи _____

3. Вихідні данні до роботи: $I_н$ = 110 А; $U_н$ = 380 V; додаткові контакти: бічний нормально відкритий 1, бічний замикальний 1, фронтальний розмикальний 1, $N_{ел}$ = $2 \cdot 10^6$.

4. Зміст розрахунково–пояснювальної записки (перелік питань, що їх належить розробити): 1. Техніко-економічне обґрунтування проекту; 2. Розрахунок струмоведучих елементів контуру; 3. Конструювання механізму апарату; 4. Попередній розрахунок електромагніту; 5. Розрахунок системи дугогасіння; 6. Розрахунок пружин; 7. Моделювання у програмі FEMM.

5. Перелік графічного матеріалу (з точним визначенням обов’язкових креслень):
СЕМ 80-220, електрична схема, передня кришка, шина, болт, корпус котушки, пластина.

6. Консультанти розділів роботи

Розділ	ПРІЗВИЩЕ, ініціали та посада консультанта	Підпис, дата	
		завдання видав	прийняв виконане завдання
1-8	БЛИЗНЯКОВ О.В., доцент		

7. Дата видачі завдання «__2__» _____вересня_____ 2024 року.

КАЛЕНДАРНИЙ ПЛАН

№ з/п	Назва етапів магістерської роботи	Строк виконання етапів роботи	Примітка
1	Огляд дизайну, вибір аналога	1 тиждень	
2	Розрахунок струмоведучих елементів контуру	2-3	
3	Конструювання механізму апарату	4	
4	Попередній розрахунок електромагніту	5	
5	Розрахунок системи регулювання дуги, розрахунок пружин	6	
6	Моделювання електромагніту, проведення дослідів.	4	
7	Виконання креслень	7-8	
8	Оформлення пояснювальної записки	9	

Студент(ка) _____ Кирило НЕВТИРЯ
(підпис) (Ім'я ПРІЗВИЩЕ)

Керівник роботи _____ Олександр БЛИЗНЯКОВ
(підпис) (Ім'я ПРІЗВИЩЕ)

РЕФЕРАТ

ПЗ: 90 с., 25 рис., 3 табл., 16 джерел.

МАГНІТНИЙ ПУСКАЧ, КОНТАКТОР ЗМІННОГО СТРУМУ, ШИНИ, СТРУМОВЕДУЧИЙ ЛАНЦЮГ, ТЕМПЕРАТУРА, КОМУТАЦІЙНІ КОНТАКТИ, ЕЛЕКТРОМАГНІТ, ПРУЖИНА, ЗАХИСТ ВІД ПЕРЕВАНТАЖЕННЯ, МОДЕЛЮВАННЯ, ДОСЛІДЖЕННЯ.

Об'єкт дослідження – електромагнітний привід контактора змінного струму 380 В, 110 А на номінальну напругу 380 В та номінальний струм 110 А.

Мета роботи – розрахунок, проектування та дослідження контактора змінного струму із вказаними вище параметрами.

Методи дослідження – вибір конструктивних форм на основі існуючих заводських аналогів, розрахунок та уточнення обраної конструкції за допомогою методики із джерела [4], програмне дослідження із застосуванням програмного забезпечення FEMM, методологічні підходи до розробки, викладені у джерелі [16].

Робота здійснює широкий спектр методів дослідження, зокрема детальний аналіз технічної літератури, галузевих стандартів і моделювання роботи контактора в різних сценаріях. Проведений аналіз продемонстрував, що розроблений контактор демонструє високу ефективність та надійність при ініціації та регулюванні роботи двигунів. Запропонована система забезпечує захист двигуна від надмірного струму, що мінімізує ризик пошкоджень та сприяє стабільній роботі обладнання. Крім того, оптимізовані технічні параметри дозволили значно знизити частоту перерв у роботі, гарантуючи таким чином стабільну роботу і підвищену енергоефективність.

Розроблений контактор змінного струму на 380 В і 110 А є передовим рішенням, що не лише підвищує енергетичну ефективність, але й забезпечує надійний захист двигунів у промислових та побутових умовах. Завдяки вдосконаленій конструкції пристрій мінімізує ризики перевантаження та забезпечує безперервну роботу системи.

ABSTRACT

EN: p. 90, 25 fig., 3 tab., 16 sources.

MAGNETIC STARTER, AC CONTACTOR, BUSBARS, CURRENT-CARRYING CIRCUIT, TEMPERATURE, SWITCHING CONTACTS, ELECTROMAGNET, SPRING, OVERLOAD PROTECTION, MODELING, RESEARCH.

Object of the study – the electromagnetic drive of an AC contactor rated for 380 V and 110 A, designed to operate at a nominal voltage of 380 V and nominal current of 110 A.

Purpose of the work – calculation, design, and analysis of an AC contactor featuring the above parameters.

Research methods – selection of structural forms based on existing factory analogs, calculation, and refinement of the chosen design using the methodology from source [4], software research using FEMM software, methodological approaches to development described in source [16].

The study employs a wide range of research methods, including an in-depth review of technical literature, relevant industry standards, and modeling the contactor's operation in various scenarios. The analysis demonstrated that the developed contactor shows high efficiency and reliability in initiating and regulating motor operation. The proposed system ensures motor protection against excessive current, minimizing the risk of damage and promoting stable equipment operation. Additionally, the optimized technical parameters significantly reduced the frequency of interruptions, thus ensuring stable operation and improved energy efficiency.

The developed AC contactor rated at 380 V and 110 A is an advanced solution that not only increases energy efficiency but also ensures reliable motor protection in industrial and domestic applications. Thanks to its improved design, the device minimizes overload risks and ensures uninterrupted system operation.

CONTENTS

INTRODUCTION

A remotely controlled switching device engineered for managing high-power and inductive AC loads called contactor. Its main advantage is the ability to interrupt the current flow at multiple points simultaneously, setting it apart from electromagnetic relays, which usually interrupt the current at only one poin.

The primary applications of contactors include controlling electric motors in both residential and industrial environments, as well as facilitating the switching of circuits for reactive power compensation.

A contactor’s main components consist of contact and arc-extinguishing assemblies, an electromagnetic actuator, and an auxiliary contact system. In electromagnetically driven contactors, both primary and auxiliary contacts are directly linked to the electromagnet's armature, which governs the closing coil.

Widely used in industrial settings, contactors manage a range of electrical loads, including machinery, lighting circuits, heating systems, power factor correction equipment, climate control systems, and other electrical devices. They come in a broad array of sizes, from compact, handheld models to larger units with dimensions of about one meter (or three feet) per side.

Beyond their primary switching functions, electromagnetic contactors also provide protection against voltage drops in the network. Should the voltage fall below a specified level, the electromagnet loses its capacity to hold the contactor in position, resulting in an automatic shutdown.

This project is dedicated to the calculation, design, and analysis of an AC contactor with a DC electromagnet, rated at 110 A and 380 V.

1 FEASIBILITY STUDY OF THE PROJECT

1.1 Design overview

The primary function of an AC contactor is to manage the switching of electrical loads on and off. These contactors are versatile and can be integrated into various equipment types, including starters, control stations, and switching devices, available in configurations that are drip-proof, splash-proof, waterproof, hermetically sealed, and explosion-proof.

Numerous contactors and magnetic starters are available with rated specifications of 380 V and 110 A. To facilitate a comprehensive understanding of the construction, refer to fig. 1.1 [11].

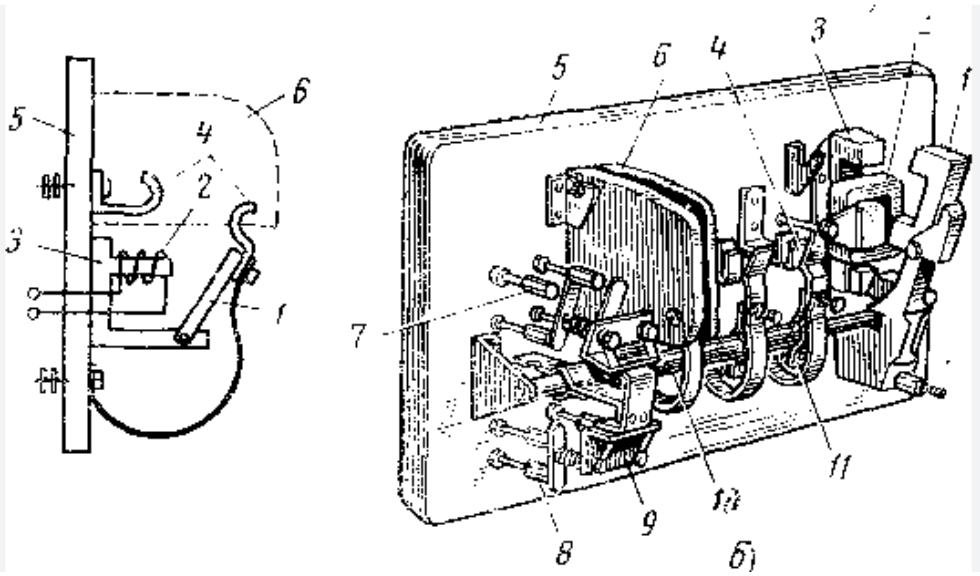

Figure 1.1 – An overview of the KT series three-pole AC contactor

a - the operation of the system; b - the overall appearance of a three-pole AC switching device; 1 - electromagnet armature; 2 - retraction coil; 3 - electromagnet core; 4 - the stationary contacts of power circuit; 5 insulation plate; 6 - arc extinguishing chambers; 7, 8 - stationary contact blocks; 9 - traverse of the movable contact blocks; 10 - roller of the moving contacts in the electrical power circuit; 11 - sliding contacts of the electrical power circuit.

ABB’s AF series of contactors, featuring an innovative AC/DC control coil, establishes a new benchmark for electrical equipment manufacturers. These advanced coils manage significant power loads efficiently, while the contactors themselves monitor and respond to power fluctuations dynamically.

The AF series includes integrated electronic control boards capable of detecting variations in supply voltage, allowing precise control over contactor engagement and disengagement. Additionally, the AF technology adjusts background current to ensure quiet, vibration-free operation.

Figure 1.2 illustrates the construction for better clarity [14].

Figure 1.2 – ABB AF65-30-00-13 Contactor 105A, 400V, AC

The KTI series electromagnetic contactors are engineered for control circuits that start and stop three-phase asynchronous motors with squirrel-cage rotors in AC networks with voltages up to 660 V. They are versatile and can also control other electrical systems, including lighting, heating units, and various inductive loads. These contactors are frequently employed in applications such as fans, pumps, furnaces, overhead cranes, and Automatic Transfer Systems (ATS).

Designed to meet the international standards of IEC 60947-4-1-2000, KTI series contactors offer several advantages:

A straightforward design that facilitates easy component replacement, particularly the retracting coil.

A base constructed from aluminum profile, delivering enhanced durability and reduced weight compared to comparable models.

Refer to figure 1.3 in [13] for additional insights.

Figure 1.3 – KTI -5115 400B 115A /AC3 IEK

1.2 Selection of an Analogue

After evaluating various domestic and international options, the CEM80.00-220V-DC contactor was chosen.

A contactor is an electromagnetically operated device designed for the frequent remote switching of AC and DC electrical circuits. It provides a reliable and safe solution for starting electric motors under heavy load conditions. Contactors equipped with

thermal relays function similarly to magnetic starters. Refer to figures 1.4, 1.5, and 1.6 [12] for images of the contactor.

Figure 1.4 – CEM80.00-220V-DC contactor

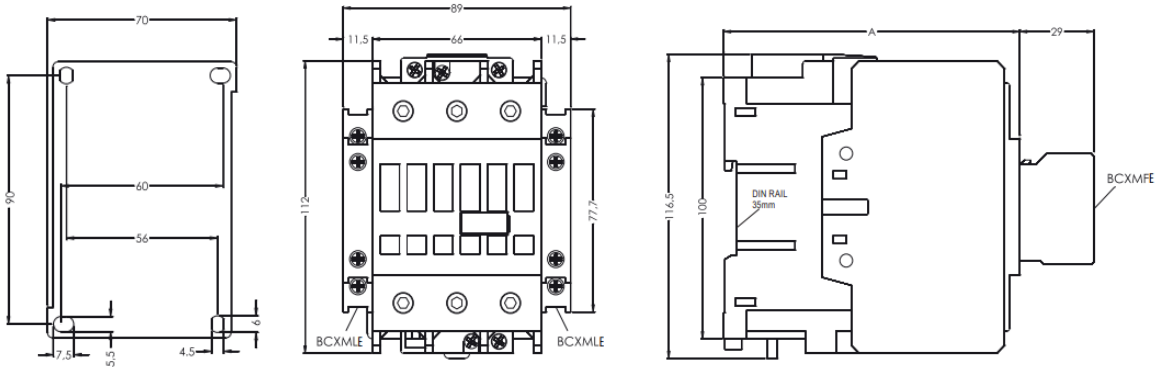

Figure 1.5, 1.6 – Overall, the mounting and connection dimensions of the CEM80.00-220V-DC contactor

1.3 Comprehensive description of the chosen analog

The selected contactor is from the CEM series, specifically model CEM80.00-220V, which features the following specifications:

- contacts type: 3NO;
- mode of operation: Continuous;
- rated operating current (AC-1) I_n,: 110 A;
- volume: 0.00130 kg;
- voltage of control coil U: 220V;
- nominal voltage U_n: 380V;
- additional contacts type: 1NO+1NC;
- application classification: AC-1, AC-3;
- weight: 1.13 kg;
- protection degree: IP20;

Climatic requirements for contactor operation:

- ambient humidity level: less than 98% at temperatures up to 40 °C;
- ambient temperature range -15…+45 °C;
- Capable of withstanding mechanical loads;
- Resistance to precipitation, including hoarfrost accumulation and melting in the off-state.

This contactor is intended for use in stationary installations for remotely starting, stopping, and reversing asynchronous motors with squirrel-cage rotors operating at AC voltages up to 1000 V. The power supply coil can be replaced to accommodate other nominal voltages, and the option to add side contact blocks helps to conserve cabinet space.

It offers the flexibility to replace the coil power supply with other nominal voltage values and features the option for side-mounted contact blocks, optimizing space and reducing cabinet depth.

The contactor is compatible with microprocessor-based control systems and allows for bridging with interference suppression devices or thyristor control. Its compact design, cost-effectiveness, simplicity of operation, and adjustable parameters make it ideal for use in the apparatus construction and calculations for this project.

2 CALCULATION OF CURRENT-CARRYING CIRCUIT ELEMENTS

Initial data for current-carrying circuit design:

- Rated current, I_n: 110 A;
- Rated voltage, U_n: 380 V;
- Tripping frequency, Z: 1200 tripping/hour;
- Maximum breaking current, I_{br} is $8I_n$ A;
- Switching life, N_{el}: 1.1 million cycles.

The objective of these calculations is to determine the appropriate cross-sectional dimensions for the current-carrying circuit, resistance of materials, transient resistance of contact points, voltage drop, and both thermal and dynamic resistance. Additionally, it is essential to ensure that temperatures within the circuit elements do not exceed permissible values and that the contact pressure is adequate to avoid welding or accidental opening under electro-dynamic forces.

The current-carrying circuit for the AC magnetic starter of the selected type is shown in figure 2.1.

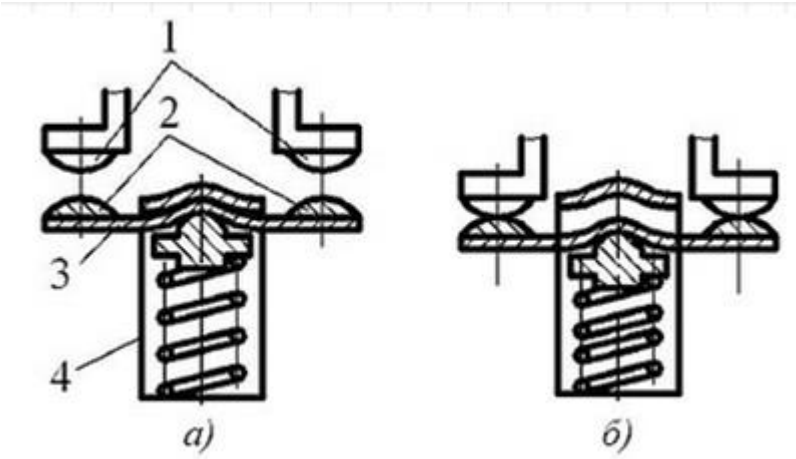

Figure 2.1 – The current-carrying circuit of the magnetic starter

1– fixed contacts, 2 – movable contacts, 3 – contact plate, 4 – contact spring.

Current-carrying component calculations are conducted for two operating conditions: continuous rated current flow, I_n and short-term flow of maximum breaking current, I_{br}.

2.1 Output Bus Calculations

The dimensions of non-insulated, current-carrying conductors are determined using Newton's formula [3; 5]:

$$p \cdot q = \frac{{I_n}^2 \cdot \rho_0 \cdot (1+\alpha_c \cdot \vartheta_c) \cdot k_{\text{add\_losses}}}{k_t \cdot (\vartheta_c - \vartheta_{\text{env}})}, \quad (2.1)$$

where p is the perimeter of the conductor's cross-
section, in cm, participating in heat exchange with the environment;

S is the cross-sectional area of the conductor, in cm²;

ρ_0 is specific electrical resistance at 0 ^{0}C; ρ_0 is equal $1.62 \cdot 10^{-6}$ Ohm·cm;

a is the temperature coefficient of resistance; a is equal $4.3 \cdot 10^{-3}$ 1/deg;

ϑ_c is the allowable continuous operating temperature of the conductor (as per ГОСТ 403-73); $\vartheta_c = 105^0$C;

K_{ad} is the additional loss coefficient due to skin and proximity effects, $K_{ad} = 1$;

ϑ_{env} is the ambient temperature, usually $\vartheta_{env} = 40\ ^0$C;

K_T is the heat transfer coefficient, $K_T = 7$ Wt/cm^2 · deg.

$$p \cdot q = \frac{110^2 \cdot 1.62 \cdot 10^{-6} \cdot (1 + 4.3 \cdot 10^{-3} \cdot 105) \cdot 1}{7 \cdot 10^{-4} \cdot (105 - 40)} = 0.6253 \text{ cm}^3.$$

For a non-insulated, rectangular busbar with sides a and b taking into account m = a / b, when pq = 2m(1+m)b^3

$$b = \sqrt[3]{\frac{\left(I_n{}^2 \cdot \rho_0 \cdot k_{add\_losses} \cdot (1+\alpha_c \cdot \vartheta_c)\right)}{2 \cdot m \cdot (m+1) \cdot k_t \cdot (\vartheta_c - \vartheta_{\text{env}})}}, \quad (2.2)$$

where m is ratio between sides of the bus; m is 0.2;

K_{ad} is equal to 1.

$$b = \sqrt[3]{\frac{\left(110^2 \cdot 1.62 \cdot 10^{-6} \cdot 1 \cdot (1 + 4.3 \cdot 10^{-3} \cdot 105)\right)}{2 \cdot 0.2 \cdot (0.2 + 1) \cdot 7 \cdot 10^{-4} \cdot (105 - 40)}} = 1.0922 \text{ cm}.$$

The value of size a can be found from expression m = a / b

$$a = m \cdot b, \quad (2.3)$$

$$a = 0.2 \cdot 0.8632 = 0.2184 \text{ cm}.$$

The bus cross-sectional area is calculated by next formula

$$S = a \cdot b, \quad (2.4)$$

$$S = 0.1767 \cdot 0.8833 = 0.2386 \text{ cm}^2.$$

According to ГОСТ 434-78 the nearest standard cross-sectional area for the bus S and standard values of dimensions a and b are chosen

$$S = 0.275\text{cm}^2;\ a = 0.25 \text{ cm};\ b = 1.1 \text{ cm}.$$

For the selected cross-sectional dimensions, the steady-state heating temperature of the bus is determined by the following formula:

$$\vartheta_{\text{set}} = \vartheta_{\text{env}} + \frac{\rho_0 \cdot (1+\alpha_c \cdot \vartheta_c) \cdot {I_n}^2 \cdot k_{\text{add\_losses}}}{k_t \cdot S \cdot p}, \quad (2.5)$$

where p represents the perimeter of the bus cross-section, calculated as:

$$\text{p} = 2 \cdot (\text{a} + \text{b}), \quad (2.6)$$

$$\text{p} = 2 \cdot (0.2 + 1) = 2.7 \text{ cm}.$$

Steady-state heating temperature of a bus (2.5)

$$\vartheta_{\text{set}} = 40 + \frac{1.62 \cdot 10^{-6} \cdot \left(1+4.3 \cdot 10^{-3} \cdot 105\right) \cdot 80^2 \cdot 1}{7 \cdot 10^{-4} \cdot 0.2 \cdot 2.4} = 94.7423\ ^0\text{C}.$$

The calculated steady-state heating temperature, ϑ_{set} = 94.7423 ^{0}C, , remains below the permissible long-term heating limit of ϑ_c = 105^{0}C (ГОСТ 434-70), affirming the accuracy of the calculation..

The verified bus cross-section is then evaluated for thermal stability under the maximum breaking current I_{br}. To assess the thermal endurance, the thermal impulse parameter $I^2_{br}\ t_{sc}$ is calculated as follows:

$$A_{\text{th\_s}} = \frac{\gamma \cdot C \cdot S^2 \cdot \ln\left(\frac{1+\alpha_C \cdot \vartheta_{\text{sc}}}{1+\alpha_C \cdot \vartheta_C}\right)}{\rho_0 \cdot \alpha_C \cdot k_{\text{add\_losses}}}, \quad (2.7)$$

$$A_{\text{th\_s}} = \frac{8.94 \cdot 0.39 \cdot 0.275^{\,2} \cdot \ln\left(\frac{1 + 4.3 \cdot 10^{-3} \cdot 300}{1 + 4.3 \cdot 10^{-3} \cdot 105}\right)}{1.62 \cdot 10^{-6} \cdot 4.3 \cdot 10^{-3} \cdot 1} = 1.7259 \cdot 10^7\ A^2 \cdot s.$$

where γ is the density of the bus material, γ = 8.94 g/cm^3;

C is the specific heat capacity, C = 0.39 J/g · deg;

ϑ_{sc} and ϑ_c is are the allowable heating temperatures of the bus in short-circuit and continuous modes, respectively, set at 300^0C and 105 ^{0}C.

Finally, the thermal stability duration is determined by the following formula:

$$t_{sc} = \frac{A_{th\_s}}{I_{br}{}^2}, \tag{2.8}$$

$$t_{sc} = \frac{1.7259 \cdot 10^7}{660^2} = 39.6203\ s.$$

The obtained thermal stability value must be at least 5 s.

2.2 Calculation of bolt requirements

In control switchgear, contact connections are critical for securing busbars, which prevents displacement of conductors and shields the device from multiple operational issues. According to failure statistics, a significant number of breakdowns occur within these contact nodes. For instance, inadequate contact can lead to excessive heat generation at the connection, potentially causing localized melting, conductor detachment, and other malfunctions.

The calculation for a dismountable contact connection involves determining the necessary contact area and calculating the number and size of bolts required to maintain adequate contact pressure. Following this, a validation of the contact connection parameters is conducted. The structure of the dismountable contact connection is illustrated in figure 2.2.

Figure 2.2 – Design of a detachable contact connection

The area of the contact surface at the bus duct connection can be calculated using the following formula:

$$S_{\text{cont}} = l \cdot b = \frac{I_{\text{n}}}{J_c}, \tag{2.1}$$

where is the overlap length of the bus;

b is the width of the bus, equal to 0.011 m;

J_c represents the theoretical current density for the copper bus.

For a nominal current of 110 A per bus duct, the current density in the designed contact connection is selected according to the following condition:

$$J_c = \left(0.31 - 1.05 \cdot 10^{-4} \cdot (I_{\text{n}} - 200)\right) \cdot 10^6, \tag{2.2}$$

$$J_c = 3.1945 \cdot 10^5 \ \frac{A}{mm^2}.$$

Let's proceed with calculating the area of the contact surface using formula (2.1):

$$S_{\text{cont}} = \frac{1575}{1.6563 \cdot 10^5} = 0.0003 \ m^2$$

The overlap length of the busbars at their connection point can be calculated as follows:

$$l = \frac{s_{\text{cont}}}{b}, \tag{2.3}$$

$$l = \frac{0.0095}{0.011} = 0.0003\ m$$

For the connection of flat busbars, it is recommended that the overlap length be set equal to the width of the busbar, assuming it allows for the placement of the required number of bolts. Based on this recommendation, an overlap length of 0.016 m is selected. Therefore, the area of the contact surface is calculated as:

$$S_{\text{cont1}} = b \cdot b_1, \tag{2.4}$$

$$S_{\text{cont1}} = 0.011 \cdot 0.016 \ = 0.0002\ \text{m}^2.$$

The required number of bolts is determined by the necessary contact pressure force F_k, given by the condition:

$$F_{\text{cont}} = f_{\text{cont}} \cdot s_{\text{cont1}}, \tag{2.5}$$

where f_{cont} is the contact pressure force per unit area, equal to $9.81 \cdot 10^6$ N/m^2 for copper.

$$F_{\text{cont}} = 9.81 \cdot 10^6 \cdot 0.0155 = 1.7265 \cdot 10^5\ N$$

The calculated number of bolts n can be determined by:

$$n = \frac{F_{\text{cont}}}{F_\delta}, \tag{2.6}$$

where F_δ is the force exerted by a single bolt, which for a selected M6 bolt is

$9.81 \cdot 10^6\ N$.

$$n = \frac{1.7265 \cdot 10^5}{9.81 \cdot 10^6} = 0.5954$$

Considering the structural characteristics of the busbar and design recommendations, a single bolt is selected to meet the force requirements for secure connection.

2.3 Contact connections

The chosen view for dismountable contact connections is shown in figure 2.3:

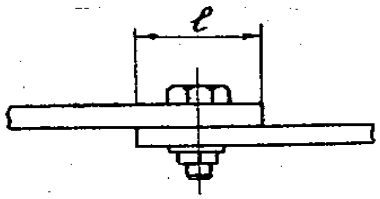

Figure 2.3 – The appearance of contact connection

The temperature at the contact point can be calculated using:

$$\vartheta_{\text{cont}} = \vartheta_{\text{set}} + \frac{{I_n}^2 \cdot R_{\text{cont}}}{k_t \cdot (S_{\text{c1}} - S_{\text{bolt}})}, \quad (2.7)$$

where R_{cont} is the total resistance of the contact connection;

S_{c1} is the area of the total external surface of the contact connection;

S_{bolt} is the cross-sectional area of the chosen bolt.

The total resistance of the contact connection R_{cont} includes the transient resistance R_c of the contact and the ohmic resistance R_{c1} of the conductor parts:

$$R_{cont} = R_c + R_{c1}\,. \tag{2.8}$$

Transient resistance Rc can be determined by:

$$R_c = \frac{\varepsilon_{sur}}{m_1 \cdot {P_k}^{m_2}}, \tag{2.9}$$

where ε is a material-specific factor, with a value of $0.24 \cdot 10^{-2}$ Ohm·N;

m_1 is the number of bolts in the connection;

P_c is the contact pressure force, N;

m_2 is a factor based on contact type, with a value of 0.85 for two-dimensional contacts.

The contact pressure force P_k is determined by recommended values of specific contact pressure p_k and by the area of contacting surface S_c:

$$P_c = p_k \cdot S_{c.} \tag{2.10}$$

where p_c is the specific contact pressure, which for copper is 600 N/cm^2.

S_c is the contact area, calculated as:

$$S_c = \frac{I_n}{J_m}, \tag{2.11}$$

Given J_m = 0.31 A/mm^2 for copper buses with an AC current below 200 A, the contact surface area is:

$$S_c = \frac{110}{0.31 \cdot 100} = 3.5484\text{cm}^2.$$

Thus, the contact pressure force is:

$$P_{\text{k}} = 600 \cdot 3.5484 = 2129.0323 \text{ N}.$$

With P_k selecting a single M6 bolt satisfies the recommended pressure (2.9 kN > 1.5 kN), $m_1 = 1$ [4].

We can now determine R_c:

$$R_c = \frac{0.24 \cdot 10^{-2}}{1 \cdot 2129.0323^{0.85}} = 3.5584 \cdot 10^{-6}\ Ohm.$$

Resistance R_{c1} differs from resistance of a straight line section of contacting parts because of current lines curvature at the contact point. It is taken into account by correction factor K_c, specified by the dependence $K_c = f(\frac{1}{a})$ in [4].

The resistance R_{c1} of the conductor parts, taking into account current path curvature, is calculated as:

$$R_{\text{c1}} = k_c \cdot \frac{\rho_0 \cdot l}{k_t \cdot (S_{\text{c}} - S_{\text{bolt}})}, \quad (2.12)$$

where S_{bolt} is the cross-sectional area of the bolt, calculated as $\frac{2 \cdot \pi \cdot d^2}{4}$;

l is the length of the contact connection (2.726 cm);

ρ_0 is the specific electrical resistance ($1.62 \cdot 10^{-6}$ Ohm·cm);

$$S_{\text{c1}} = S_c - S_{\text{bolt}} \text{ cm}^2,$$

where S_c is the contact surface area as calculated in formula (2.3);

d is the diameter of an M6 bolt from table in [4], equal to 0.65 cm;

$$S_{\text{c1}} = 3.5484 - 2 \cdot 3.14 \cdot \frac{0.4225^2}{4} = 2.8851 \text{ cm}.$$

$$K_c = f(\frac{1.9173}{0.18}) = f(10.651) = 0.55.$$

The resistance R_{c1} of the conductor parts, taking into account current path curvature, is calculated as:

$$R_{c1} = 0.55 \cdot \frac{1.62 \cdot 10^{-6} \cdot 2.726}{7 \cdot 10^{-4} \cdot 2.8851} = 8.4188 \cdot 10^{-7} \text{ Ohm}.$$

To determine the total resistance of the contact connection, R_{cont} the transient resistance of the contact R_c and the ohmic resistance R_{c1} of the conductor parts are substituted into the formula (2.12)

$$R_{cont} = 3.5584 \cdot 10^{-6} + 8.4188 \cdot 10^{-7} = 4.4003 \cdot 10^{-6} \text{ Ohm}.$$

With this value calculated, we can now determine the temperature at the contact point, ϑ_{cont}, using formula (2.7):

$$\vartheta_{cont} = 94.7423 + \frac{110^2 \cdot 4.4003 \cdot 10^{-6}}{7 \cdot 10^{-4} \cdot 2.8851} = 121.1064\ ^{\circ}C\,.$$

2.4 Switching contacts

The purpose of this calculation is to determine the necessary contact pressure force to keep the contact point temperature within safe limits and to prevent issues such as welding and unintended contact opening due to electrodynamic forces.

For high durability, ceramic metal (cermet) is recommended as the material for contact plates. Though this choice may increase initial costs, ceramic metal contacts offer excellent arc stability, which greatly enhances the reliability and lifespan of the apparatus, making the investment worthwhil.

In designing the AC contactor, silver with cermet was selected for the contact plates. For bridge contacts, the width of the movable contact should be equal to or up to 25% wider than the width of the current-carrying bus or flexible connection.

The width of the movable contact, $b_{\text{m\_c}}$, is calculated as follows:

$$b_{\text{m\_c}} = 1.2 \cdot b, \tag{2.13}$$

$$b_{\text{m\_c}} = 1.2 \cdot 1{,}1 = 1.32 \text{ cm}.$$

The nearest standard value for the width of the movable contact, $b_{m.c}$ is selected as 1.044 cm in accordance with ГОСТ 3884-67.

The length of the movable contact, l, is set at 2 cm.

The perimeter of the movable contact is calculated using the formula:

$$p_1 = 2 \cdot \left(l + b_{\text{m\_c}}\right), \tag{2.14}$$

$$p_1 = 2 \cdot (2 + 1.32) = 6.64 \text{ cm}.$$

The section of the contact details along the contact line is defined by:

$$S_{\text{m\_c}} = l \cdot b_{\text{m\_c}}, \tag{2.15}$$

$$S_{\text{m\_c}} = 2 \cdot 1.32 = 2.64 \text{ cm}^2.$$

In continuous mode with a rated current I_n , the transient contact resistance, accounting for the influence of the electric arc on contact heating, is represented by the expression [4]:

$$S_{\text{m\_c}} = l \cdot b_{\text{m\_c}}, \tag{2.16}$$

$$\vartheta_m - \vartheta_{env} = \vartheta_{set} + \frac{R_{tr\_c} I_n^2 + \mathrm{P}_{el.arc}}{2\sqrt{\lambda K_T p_1 S}_{m\_c}} + \frac{R_{tr\_c}^2 \cdot I_n^2}{8\lambda\rho_0(1+\alpha\vartheta_{set})}, \qquad (2.17)$$

where ϑ_m is the maximum temperature of the contact surface, °C;

ϑ_c is the temperature of the contact detail (94.7423 °C);

S_{m_c} is the cross-sectional area of the contact details along the contact line (2.64 cm²);

$P_{el.arc}$ denotes the portion of power losses due to the presence of the electric arc in the apparatus contacts (in Watts);

λ is the thermal conductivity coefficient of the contact plate material, $\lambda = 4.16 \frac{\mathrm{Wt}}{\mathrm{cm}\cdot°\mathrm{C}}$.

The power losses attributed to the electric arc in the apparatus contacts can be calculated using the formula:

$$P_{el.arc} = \frac{0{,}1 \cdot U_a \cdot I_a \cdot t_a \cdot Z}{3600}, \qquad (2.18)$$

where U_a is the arc voltage (in Volts);

I_a is the arc current (in Amperes);

t_a is the duration of the arc burn on the contacts (in seconds).

For the calculation of the AC arc blow-out device, the duration of the arc burn t_a is taken as 0.0015 s, and the arc voltage U_a is estimated between 0.5 and 0.8 of the rated voltage U_n with U_a set at 247 V.

The arc current is determined as follows:

$$I_a = \frac{I_n}{2}, \qquad (2.19)$$

$$I_a = \frac{110}{2} = 55 \text{ A}.$$

Substituting the known values into this equation (2.19), the power losses due to the electric arc in the apparatus contacts can be calculated as:

$$P_{el.arc} = \frac{0{,}1 \cdot 247 \cdot 55 \cdot 0.0015 \cdot 1200}{3600} = 0.6792$$

The contact pressure force is defined by the expression:

$$P_{c1} = \rho_{sp} \cdot I_n, \quad (2.20)$$

where ρ_{sp} – is the specific contact pressure per ampere of rated current (N/A). For silver contacts in contactors, this value is typically between 0.07 and 0.145 N/A.

$$P_{c1} = 0.1 \cdot 110 = 11 \text{ N}.$$

The transient contact resistance R_{tr_c} is calculated using the formula:

$$R_{tr.c} = K_1 \cdot \frac{1+\frac{2}{3}\cdot(\vartheta_{set}\cdot\alpha_c+1)}{(0.102\cdot P_{c1})^{m_{coef}}}, \quad (2.21)$$

where K_1 and m empirical coefficients selected based on the contact material and type, as specified in [3]. Here, K_1 = 0.00006 m.

$$R_{tr\_c} = \frac{0.00006\cdot\left(1+\frac{2}{3}\cdot 0.0043\cdot 94.7423\right)}{(0.102\cdot 11)^1} = 0.0001 \text{ Ohm}.$$

The accuracy of the contact pressure force calculation is verified by ensuring the contact surface temperature ϑ_{cs} does not exceed the maximum temperature ϑ_m

$$\vartheta_{cs} = \vartheta_{set} + \frac{R_{tr\_c} \cdot {I_n}^2 + P_{el\_arc}}{2 \cdot \sqrt{\lambda \cdot k_t \cdot p_1 \cdot S_{m\_c}}} + \frac{{R_{tr\_c}}^2 \cdot {I_n}^2}{8 \cdot \rho_0 \cdot \lambda \cdot (1 + \alpha_c \cdot \vartheta_{set})}, \quad (2.22)$$

$$\vartheta_{cs} = 94.7423 + \frac{0.0001 \cdot 110^2 + 0.6792}{2\sqrt{4.16 \cdot 7 \cdot 10^{-4} \cdot 6.64 \cdot 2.64}} + \frac{0.0001^2 \cdot 110^2}{8 \cdot 4.16 \cdot 1.62 \cdot 10^{-6} \cdot (1 + 0.0043 \cdot 94.7423)} = 100.7342°C.$$

In the short-term fault condition with a current $I_{s.c}$ it's necessary to verify that the calculated contact pressure P_{c1} prevents contact welding. The welding current is I_{welding} given by.

Welding current is calculated by the following formula

$$I_{\text{welding}} = \sqrt{\frac{\lambda \cdot P_{c1} \cdot (\vartheta_{\text{melt}} - \vartheta_{cs})}{0.1 \cdot \rho \cdot \sigma_{sm}} \cdot \exp\left(\frac{C \cdot \gamma}{\lambda} \cdot \sqrt{\frac{P_{c1}}{3.14 \cdot \sigma_{sm} \cdot t_{sc}}}\right)}, \quad (2.23)$$

where ϑ_{melt} is the melting temperature of the contact material, set to 961°C;

γ is the material density, γ is 10 g/cm^3 for silver with cadmium oxide;

ρ is the specific electrical resistance ($\rho = 1.59 \cdot 10^{-6}$ Ohm $\cdot$ cm) ;

C – is specific heat (J/g·deg; it is 0.234 J/g·deg);

σ_{com} is the ultimate compressive strength (σ_{com} is 30300 N/cm$^{2)}$.

$$I_{\text{welding}} = \sqrt{\frac{4.16 \cdot 11 \cdot (961 - 100.7342)}{0.1 \cdot 1.59 \cdot 10^{-6} \cdot 30300} \cdot \exp\left(\frac{0.234 \cdot 10}{4.16} \cdot \sqrt{\frac{11}{3.14 \cdot 30300 \cdot 5}}\right)} = 2.864 \cdot 10^3 A.$$

The contacts will not weld under the calculated pressure, as $I_{br} < I_w$.

To estimate the electrodynamic repulsion forces under short-circuit current, the following formula is applied [3]:

$$P_{el\_ef} = 10^{-7} \cdot {I_{\text{br}}}^2 \cdot \ln\left(\frac{S_{m\_c}}{S_0}\right) \cdot 2, \quad (2.24)$$

where S_0, the section area of the compression contact surface, is calculated by:

$$S_o = \frac{\pi \cdot {d_0}^2}{4}, \tag{2.25}$$

and the diameter d_0 of the contact area is:

$$d_o = 2 \cdot \sqrt{\frac{P_{c1}}{3.14 \cdot \sigma_{com}}}, \tag{2.26}$$

$$d_o = 2 \cdot \sqrt{\frac{11}{3.14 \cdot 30300}} = 0.0215\ cm.$$

Substituting d_0 into formula (2.26) section area of compression contact surface is obtained

$$S_o = \frac{3.14 \cdot 0.0215^2}{4} = 0.0004\ cm^2.$$

Thus, the electrodynamic force can be defined by formula (2.25)

$$\mathrm{P}_{el\_ef} = 2 \cdot 10^{-7} 660^2 \cdot ln \frac{2.64}{0.0004} = 0.7747\ \mathrm{N}.$$

For a properly designed contact system, the condition must be met:

$$\mathrm{P_{el\_ef}} < \mathrm{P_{c1}}.$$

$$0.7747\ \mathrm{N} < 11\ \mathrm{N}.$$

The opening distance β for the contactor is selected as 5 mm, based on rated current specifications.

$$\beta = 5 \text{ mm}.$$

2.5 Calculation of wear and subsequent contact closure.

The linear wear of contacts can be determined based on the number of operations, N_{el}, that the contacts must withstand. The wear factor, or follow-through, is set to be 1.5–2.5 times greater than the linear wear, as defined by the following relationship:

$$\sigma_f = 2 \cdot \sigma L \tag{2.27}$$

The approximate mass Q (in grams) of material consumed by one pair of contacts over its lifespan can be calculated with the formula:

$$Q \approx 10^{-9} \cdot K_u \cdot N_{el} \cdot {I_n}^2, \tag{2.28}$$

where K_u is an empirical coefficient based on current and contact material, determined from figure 1.3. Here, K_u is set to 0.2 g/A^2.

Using the formula (2.29), the material mass for one pair of contacts can be calculated as:

$$Q = 10^{-9} \cdot 1.1 \cdot 10^6 \cdot 110^2 = 2.662 \text{ g}.$$

The volumetric wear V of the contact material can then be found with the following expression:

$$V = \frac{Q}{\gamma_s}, \tag{2.29}$$

$$V = \frac{2.662}{10} = 0.2662 \text{ cm}^3.$$

Given the geometric dimensions of the contact, the linear wear σ_L can be determined from the volume wear V using the formula:

$$\sigma_L = \frac{V}{S_{m\_c}}, \tag{2.30}$$

$$\sigma_L = \frac{0.2662}{2.64} = 0.1008 \text{ cm}.$$

Using formula (2.28), the follow-through wear σ_f of the contacts is calculated as:

$$\sigma_f = 2 \cdot 0.1008 = 0.2017 \text{ cm}.$$

3 DESIGNING THE APPARATUS MECHANISM

Electromagnetic contactors are designed with two actuating mechanisms: an electromagnet drive for engaging the contact system and a spring system for releasing it. To calculate the electromagnet drive, it is essential to first establish the characteristics of opposing forces, which include the characteristics of the spring mechanism.

The spring mechanism is made up of contact and return springs that generate the force required to disconnect the armature from core once the electromagnetic drive is switched off. Initial parameters needed for calculating the contact and return springs include the preliminary (P_1) and final (P_2) compression forces for the contact springs, as well as the preliminary (P_{1pb}) and final (P_{2pb}) compression forces for the return springs.

To calculate P_2 and P_1 for the contact spring, determined previously contact pressure force (P'_c) must be transferred to the contact spring's axis, using a schematic with initial linear dimensions.

The reduced contact pressure force is calculated as follows:

$$P'_c = 2 \cdot P_{c1}\ , \tag{3.1}$$

where P_{c1} is the contact pressure force, $P_{c1} = 11$ N;

$$P'_c = 2 \cdot 11 = 22\ \text{N}.$$

The relationship between the preliminary P_1 and final P_2 compression forces of the contact spring can be expressed as:

$$P_1 = 0.6 \cdot P_2\ . \tag{3.2}$$

The value of P_2 is then obtained using the expression:

$$P'_c = \frac{P_1+P_2}{2} = \frac{0.6 \cdot P_2+P_2}{2} = 0.8 \cdot P_2, \tag{3.3}$$

$$P_2 = \frac{P_c'}{0.8}, \tag{3.4}$$

$$P_2 = \frac{22}{0.8} = 27.5 \text{ N}.$$

With the value of final compression P_2, the preliminary compression P_1 is determined as:

$$P_1 = 0.6 \cdot 27.5 = 16.5 \text{ N}.$$

The initial force of the pullback spring P_{1pb} is derived from the final compression force P_2, adjusted to the axis of the pullback spring. For a device with a valve-type solenoid and normally open contacts:

$$P_{1pb} = 0.3 \cdot \frac{3}{2} \cdot P_2, \tag{3.5}$$

where K is the number of main apparatus contacts; K = 1.

$$P_{1pb} = 0.3 \cdot \frac{3}{2} \cdot 27.5 = 12.375 \text{ N}.$$

The final pressure of the pullback spring P_{2pb} can be estimated as:

$$P_{2pb} = 1.3 \cdot P_{1pb}, \tag{3.6}$$

$$P_{2pb} = 1.3 \cdot 12.375 = 16.0875 \text{ N}.$$

For constructing the characteristic of opposing forces, the contact opening β, the follow-through δ_f, the preliminary P1 and final P2 compression forces of the contact

springs, and the preliminary P_{1pb} and final P_{2pb} compression forces of the pullback springs are aligned to the axis of the electromagnetic coil.

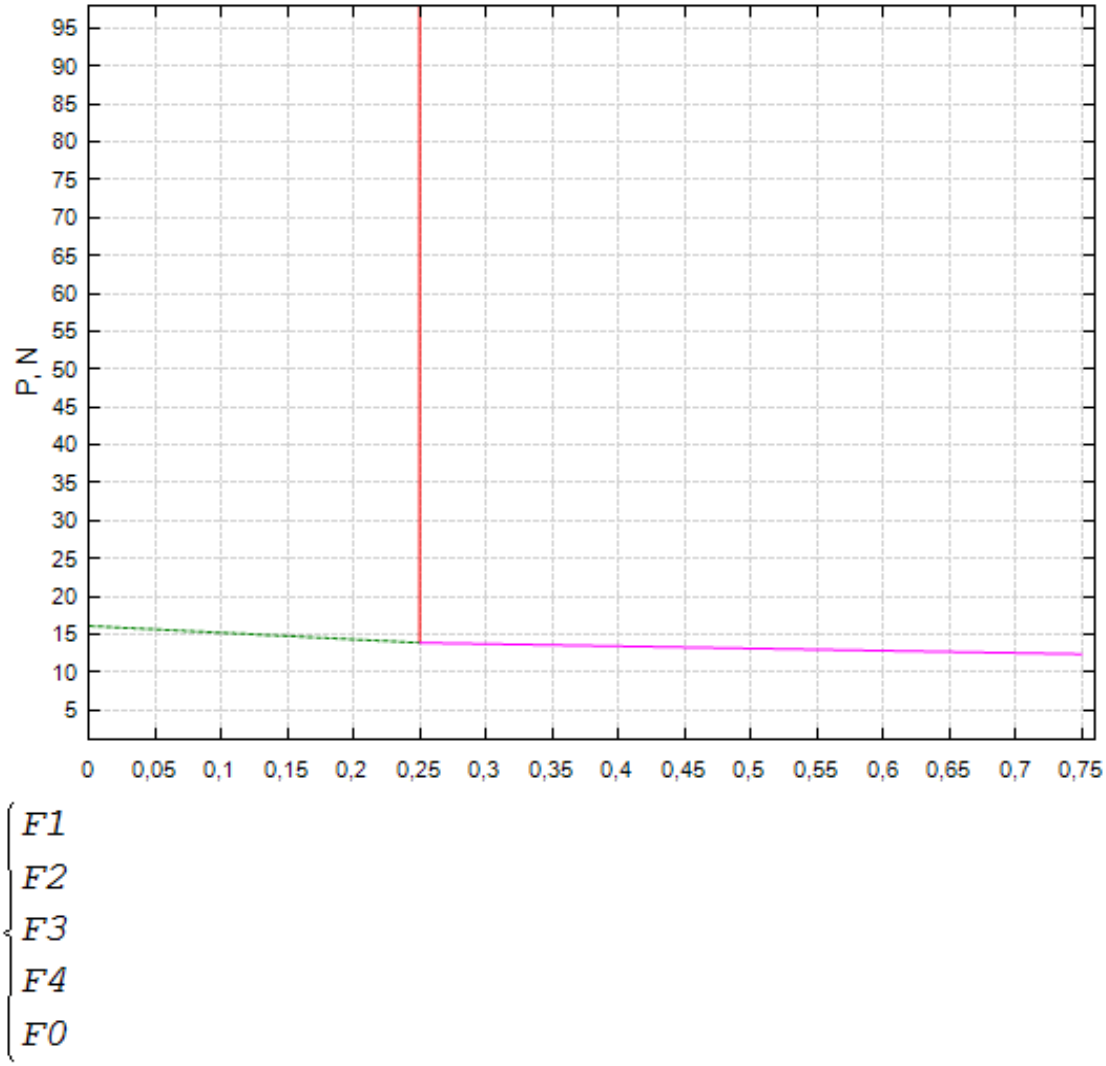

Figure 3.1 – Characteristics of the opposing forces

The force generated by the electromagnet at the critical air gap, denoted as σ'_f, is calculated using the following formula:

$$P_{\text{el\_cr}} = \left(P_{2\text{pb}} + (3 \cdot P_2)\right) \cdot K_{\text{saf}} \tag{3.7}$$

where K_{saf} is the safety factor, typically ranging between 1.3 and 1.7 for contactors;

P_{cr} represents the total opposing force value at the critical air gap.

$$P_{\text{el\_cr}} = \left(16.0875 + (3 \cdot 27.5)\right) \cdot 1.35 = \ 133.0931 \text{ N}.$$

Given that the pulling characteristic of an AC contactor is nearly linear, the point $P_{\text{el\_cr}}$ is not critical to display. Instead, the most significant point is the uppermost one on the opposing force characteristic, calculated as:

$$P_{\text{up}} = P_{2\text{pb}} + (3 \cdot P_2), \tag{3.8}$$

$$P_{\text{up}} = 98.5875 \text{ N}.$$

The initial and final forces of the contact and return springs are aligned along the coil axis as follows:

$$\text{F0} = \begin{bmatrix} 0 & P_2 \\ 0 & P_2 + 0.5 \end{bmatrix} \tag{3.9}$$

$$\text{F1} = \begin{bmatrix} 0 & P_{\text{el\_cr}} \\ a & P_{\text{up}} \end{bmatrix}$$

$$\text{F2} = \begin{bmatrix} a & P_{\text{up}} \\ a & P_{1\text{pb}} + 1.5 \end{bmatrix}$$

$$\text{F3} = \begin{bmatrix} 0 & P_{2\text{pb}} \\ a & P_{1\text{pb}} + 1.5 \end{bmatrix}$$

$$\text{F4} = \begin{bmatrix} a & P_{1\text{pb}} + 1.5 \\ a + \dfrac{\beta}{10} & P_{1\text{pb}} \end{bmatrix}$$

The pulling and opposing force characteristics are illustrated in fig. 3.1

4 PRELIMINARY CALCULATION OF THE ELECTROMAGNET

The purpose of this calculation is to preliminarily determine the dimensions of the magnetic circuit, the magnetizing force of the winding, and geometrical dimensions.

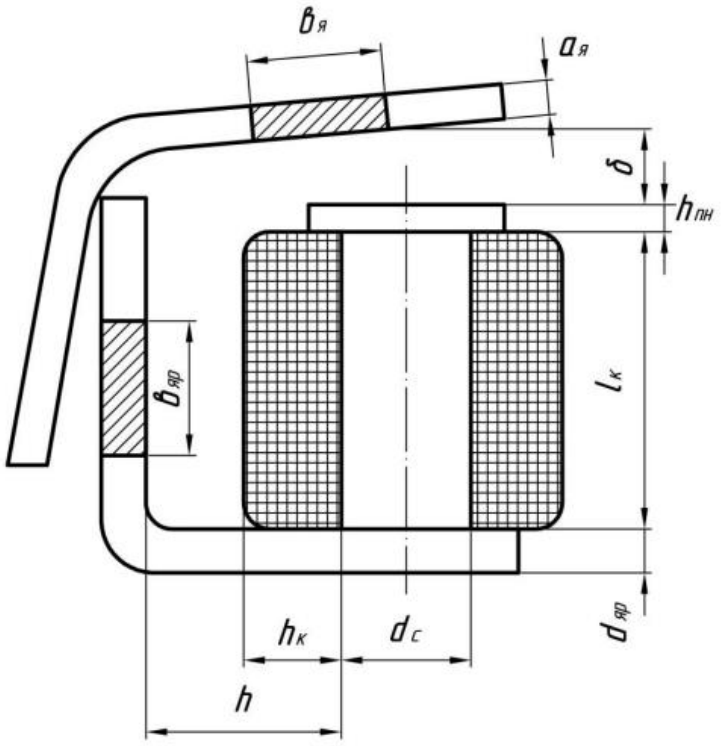

Figure 4.1 – Electric solenoid valve

For electromagnets with a pole tip, the cross-sectional area of the pole tip $S_{\text{p\_t}}$, in cm², can be determined using Maxwell's formula:

$$S_{\text{p\_t}} = \sqrt{\frac{P_{\text{el\_cr}}}{39.8 \cdot {B_\delta}^2}}, \tag{4.1}$$

where $P_{\text{el\_cr}}$ is the force the electromagnet can generate at the critical air gap σ'_f;

B_δ is the magnetic induction in the air gap, typically between 0.5 and 0.9 T.

$$S_{\text{p\_t}} = \sqrt{\frac{133.0931}{39.8 \cdot 0.5^2}} = 3.6573 \text{ cm}^2.$$

Pole tip diameter:

$$d_{\text{p\_t}} = \sqrt{\frac{4 \cdot S_{\text{p\_t}}}{\pi}}, \tag{4.2}$$

$$d_{\text{p\_t}} = \sqrt{\frac{4 \cdot 3.6573}{3.14}} = 2.1579 \text{ cm}.$$

The diameter of the core d_c is set from the ratios recommended in the literature: For small valve electromagnets, the pole tip height is typically set to 1.1 cm

Pole tip height: for small valve electromagnets, the pole tip height is 0.1 cm

Cross-sectional area of the core is given by:

$$S_c = \frac{\pi \cdot {d_c}^2}{4}, \tag{4.3}$$

$$S_c = \frac{\pi \cdot 1{,}1^2}{4} = 0.9503 \text{ cm}^2.$$

Cross-sectional area of the armature:

$$S_{\text{an}} = \frac{S_c}{\sigma_{\text{ad}}}, \tag{4.4}$$

where σ_{ad} ranges from 1.1 to 1.5 cm;

$$S_{\text{an}} = \frac{0.9503}{1.3} = 0.731 \text{ cm}^2$$

Cross-sectional area of the yoke

$$S_y \geq S_{\text{an}}, \tag{4.5}$$

$$S_y = 0.8 \text{ cm}^2$$

The width of the anchor, b_{an}, is selected to be equal to or slightly larger than the pole tip diameter, with $b_{\text{an}} = 1.47$ cm.

The anchor thickness is calculated by:

$$a_{\text{an}} = \frac{S_{\text{an}}}{b_{\text{an}}}, \tag{4.6}$$

$$a_{\text{an}} = \frac{0.731}{1.47} = 0.4973 \text{ cm}.$$

The magnetizing force of the winding, F_{aw}, for the critical gap is determined by:

$$F_{\text{aw}} = \frac{B_\delta \cdot \delta \cdot K_D}{\mu_0}, \tag{4.7}$$

where $\mu_0 = 4 \cdot \pi \cdot 10^{-7}$ is the magnetic permeability of air;

δ = is equal to $2.5 \cdot 10^{-3} cm$ represents the air gap at the critical point;

K_D= 1.3 accounts for the reduction in magnetizing force in non-working gaps and in the magnetic conductor.

$$F_{\text{aw}} = \frac{0.5 \cdot 2.5 \cdot 1.3}{4 \cdot \pi \cdot 10^{-7}} = 1293.$$

Winding dimensions are calculated according to thermal factor requirements:

$$l_k = \sqrt[3]{\frac{{F_{\text{kr}}}^2 \cdot n \cdot \rho_0 \cdot (1 + \alpha_c \cdot \vartheta_c) \cdot \text{DI} \cdot K_{\text{st}}}{2 \cdot f_0 \cdot K_T \cdot \tau_{\text{ad}}}}, \quad (4.8)$$

where n = 5 is the ratio coil length l_k to coil thickness h_k, typical for DC valve electromagnets is taken to be equal to 4 - 8;

DI = 1 duty cycle;

K_{st} – is the safety factor it equals to $1.3 - 2$;

f_0 = 0.5 the winding filling factor;

The heat transfer coefficient, K_T = 12, is selected based on the temperature rise in the winding, as shown in fig. 2.2. For a coil without a frame, the coefficient corresponds to line "a," and for a framed coil, it corresponds to line "b."

$F_{\text{kr}} = F_{\text{aw}} \cdot K_{\text{st}} = 1939$ A - is the magnetomotive force;

The temperature coefficient $\tau_{\text{ad}} = 50$.

$$l_k = \sqrt[3]{\frac{1939^2 \cdot 5 \cdot 1.62 \cdot 10^{-8} \cdot (1 + 0.0043 \cdot 105) \cdot 1 \cdot 1.5}{2 \cdot 0.5 \cdot 12 \cdot 50}} = 0.1034 \text{ cm}.$$

Coil thickness:

$$h_k = \frac{l_k}{n}, \quad (4.9)$$

$$h_k = \frac{0.1034}{5} = 0.0207 \text{ cm}.$$

Yoke width:

$$b_y = d_c + 2 \cdot h_k, \quad (4.10)$$

$$b_y = 1.1 + 2 \cdot 0.0207 = 1.1414 \text{ cm}.$$

Yoke thickness:

$$a_y = \frac{S_y}{b_y}, \tag{4.11}$$

$$a_y = \frac{0.8}{1.1414} = 0.7009 \text{ cm}.$$

A gap between yoke and winding, in the range of 0.5–1.5 cm, is recommended to minimize flux leakage.

Based on the calculated dimensions, the electromagnet sketch should be drawn, showing the specific measurements obtained for each part.

The coil is the core component of the electromagnet, generating the magnetizing force necessary for its operation. In electromagnetic contactors for both AC and DC, coils may be framed or frameless. Framed coils, however, are limited by poor thermal conductivity and significant surface losses.

For framed coils, the thickness of the insulating material walls must be considered when calculating the winding space, as this impacts the effective length and thickness of the winding, l_0 and h_0, respectively.

Winding thickness:

$$h_0 = h_k + 0.005, \tag{4.12}$$

$$h_0 = 0.0207 + 0.005 = 0.0257 \text{ cm}.$$

Average winding length for a round coil:

$$l_{\text{av}} = \pi \cdot (d_0 + h_0), \tag{4.13}$$

$$l_{\text{av}} = 3.14 \cdot (0.0215 + 0.0257) = 0.1482 \text{ cm}.$$

Diameter of round winding wire:

$$d = \sqrt{\frac{4 \cdot \rho_0 \cdot (1 + \alpha_c \cdot \vartheta_c) \cdot l_{\text{av}} \cdot F_{\text{kr}} \cdot K_{\text{st}}}{\pi \cdot U}}, \quad (4.14)$$

where the power supply voltage, U = 220

$$d = \sqrt{\frac{4 \cdot 1.62 \cdot 10^{-8} \cdot (1 + 0.0043 \cdot 105) \cdot 0.1482 \cdot 1939 \cdot 1.5}{3.14 \cdot 220}} = 0.0002 \text{ cm}.$$

From reference [4], the closest larger standard diameter of bare wire is selected, with an insulated wire diameter of d_1 = 0.000230 cm and a winding filling factor f_0 = 0.580.

Winding length:

$$l_0 = l_k + 0.005, \quad (4.15)$$

$$l_0 = 0.1034 + 0.005 = 0.1084\ cm.$$

Number of winding turns:

$$W = f_0 \cdot \frac{4 \cdot h_0 \cdot l_0}{\pi \cdot d^2}, \quad (4.16)$$

$$W = 0.580 \cdot \frac{4 \cdot 0.0257 \cdot 0.1084}{3.14 \cdot 0.0002^2} = 35029.$$

Length of the inner part of the coil:

$$l_{\text{av1}} = d_c + 2 \cdot l_k, \tag{4.17}$$

$$l_{\text{av1}} = 1.1 \cdot 10^{-2} + 2 \cdot 0.1034 = 0.2178\ cm.$$

The active resistance of the winding is calculated using the following formula:

$$R = \frac{4 \cdot \rho_0 \cdot (1 + \alpha_c \cdot \vartheta_c) \cdot l_{\text{av1}}}{\pi \cdot d^2} \cdot W, \tag{4.18}$$

$$R = \frac{4 \cdot 1.62 \cdot 10^{-8} \cdot (1 + 0.0043 \cdot 105) \cdot 0.2178}{3.14 \cdot 0.0002^2} \cdot 35029 = 3891\ Ohm.$$

Maximum current in the winding required for thermal calculations is determined as:

$$I = \frac{1.05 \cdot U}{R}, \tag{4.19}$$

$$I = \frac{1.05 \cdot 220}{3891} = 0.0594\ A.$$

The maximum power of the winding can be calculated by:

$$P = I^2 \cdot R, \tag{4.20}$$

$$P = 0.0594^2 \cdot 3891 = 13.711\ Wt.$$

The current density in the winding is determined as follows:

$$j = \frac{4 \cdot I}{\pi \cdot d^2}, \tag{4.21}$$

$$j = \frac{4 \cdot 0.0594}{3.14 \cdot 0.0002^2} = 1.2875 \cdot 10^6 A/m^2 .$$

The coil thickness is calculated by:

$$D = d_c + 2 \cdot h_k, \tag{4.22}$$

$$D = 0.011 + 2 \cdot 0.0207 = 0.0524\ cm$$

The cooling surface area of the coil must be calculated as:

$$S_{\text{cool}} = \pi \cdot D \cdot l_k, \tag{4.23}$$

$$S_{\text{cool}} = 3.14 \cdot 0.0524 \cdot 0.1034 = 0.017\ \text{cm}^2$$

The temperature rise τ_{set} above ambient is determined using Newton's cooling formula:

$$\tau_{\text{set}} = \frac{\text{P}}{\text{K}_\text{T} \cdot \text{S}_{\text{cool}}}, \tag{4.24}$$

$$\tau_{\text{set}} = \frac{13.711}{12 \cdot 0.017} = 67\ ^0\text{C}.$$

To verify the winding calculation, we ensure that:

$$\tau_{\text{set}} < \tau_{nom},$$

$$67\ ^0\text{C} < 85\ ^0\text{C}.$$

where τ_{nom} represents the permissible temperature rise above ambient, dictated by the insulation class.

For commonly used enamel-insulated wire (PEL), τ_{nom}= 85ºC.

The preliminary calculations indicate that the dimensions and thermal parameters are within acceptable limits, confirming that the selected dimensions meet the required specifications.

5 CALCULATIONS OF THE ARC CONTROL SYSTEM

The double-loop arc blowout method is an effective technique for circuit breaking in voltage ranges of 220-380V. This method satisfies the necessary requirements for constructing such a device.

Key factors influencing arc blowout include the recovery voltage and the number of interruptions in the circuit.

The recovery voltage of the contact gap is given by:

$$U_{\text{от}} = \frac{1.1 \cdot \sqrt{2} \cdot \text{U}_\text{n}}{\sqrt{3}} \cdot \text{k}_{\text{сх}} \cdot \sin \varphi, \quad (5.1)$$

where $\text{k}_{\text{сх}}$ = 1.5 is the scheme coefficient;

$\varphi = 66.5\ ^0\text{C}$ is the phase displacement angle.

$$U_{\text{от}} = \frac{1.1 \cdot \sqrt{2} \cdot 380}{\sqrt{3}} \cdot 1.5 \cdot \sin(1.161) = 469.5555\ \text{V}.$$

where $\text{f}_0$is the fundamental frequency (5,000–20,000 Hz) [4];

k_a is the amplitude coefficient.

$$\text{k}_\text{a} = \frac{U_{\text{v\_max}}}{U_{\text{от}}} \approx 1 + \text{e}^{-0.0003 \cdot \text{f}_0}, \quad (5.2)$$

$$\text{k}_\text{a} = 1 + \text{e}^{-0.0003 \cdot 7000} = 1.1225,$$

The inductance of the interrupted circuit is:

$$L = \frac{U_n \cdot \sqrt{1 - \left(\cos(\varphi)\right)^2}}{\sqrt{3} \cdot I_{\text{br}} \cdot 314}, \tag{5.3}$$

$$L = \frac{380 \cdot \sqrt{1 - 0.95^2}}{\sqrt{3} \cdot 660 \cdot 314} = 0.0003 \text{ H}.$$

The arc length is given by:

$$l_{\text{d0}} = \sqrt{{\delta_k}^2 + 12300 \cdot {I_{\text{br}}}^{\frac{2}{3}} \cdot 0.01^2}, \tag{5.4}$$

where $\delta_k = 2$ cm is the contact separation distance.

$$l_{\text{d0}} = \sqrt{2^2 + 12300 \cdot 660^{\frac{2}{3}} \cdot 0.01^2} = 9.861\ cm.$$

The active resistance of the arc is calculated as:

$$\text{R}_{\text{д}}^0 \approx 0.015 + \frac{14200}{\text{I}_{\text{br}}^2}, \tag{5.5}$$

$$R_{\text{д}}^0 \approx 0.015 + \frac{14200}{660^2} = 0.0476 \text{ Ohm}.$$

he equivalent resistance of the arc for one pole is calculated as follows:

$$\text{R}_{\text{д}} \approx \text{R}_{\text{д}}^0 \cdot \text{n} \cdot \text{l}_{\text{д}}^0, \tag{5.6}$$

where n = 2 is the number of breaks on one pole.

$$\text{R}_d \approx 0.0476 \cdot 2 \cdot 0.5 = 2.3469 \text{ Ohm}.$$

To determine if the initial number of breaks n = 2 is sufficient to extinguish the arc, the required number of breaks n_{a_cal} is recalculated using the following formula:

$$n_{a\_cal} = \frac{k_n \cdot U_n - A_x\left(1 + \ln\frac{k_n \cdot U_n}{A_x}\right)}{U^0_{v.p.} + 0.34 \cdot k_n \cdot l^0_д \cdot R^0_d \cdot I_{br}}, \quad (5.7)$$

where the coefficients k_n, A_x and M_0 are used in calculating the number of breaks needed to ensure effective arc blowout, which are

$$k_n = 0.9 \cdot k_{cx} \cdot \sqrt{1 - \cos\varphi_0}, \quad (5.8)$$

$$k_n = 0.9 \cdot 1.5 \cdot \sqrt{1 - 0.95} = 0.3019,$$

$$M_0 \approx 0.8 \cdot 10^{-5} + \frac{2.5}{I^2_{br}}, \quad (5.9)$$

$$M_0 \approx 0.8 \cdot 10^{-5} + \frac{2.5}{660^2} = 1.3739 \cdot 10^{-5},$$

$$A_x = \frac{k_\Sigma \cdot \beta_к \cdot L}{M_0}, \quad (5.10)$$

where $\beta_к = 2$, which is obtained from reference [4];

k_Σ is typically taken as 1 for this calculation.

$$A_x = \frac{1 \cdot 2 \cdot 0.0003}{1.3739 \cdot 10^{-5}} = 48.1194,$$

$$n_{a\_cal} = \frac{0.3019 \cdot 380 - 48.1194 \cdot (1 + \ln\frac{0.3019 \cdot 380}{48.1194})}{70 + 0.34 \cdot 0.3019 \cdot 9.861 \cdot 0.0476 \cdot 660} = 0.2435.$$

$$n_a > n_{a\_cal},$$

$$1 > 0.2435.$$

$$f_{0\_cal} = \frac{M_0 \cdot n_a \cdot 10^6}{\pi \cdot L}, \quad (5.11)$$

$$f_{0\_cal} = \frac{1.3739 \cdot 10^{-5} \cdot 2 \cdot 10^6}{3.14 \cdot 0.0003} = 26473 \text{ Hz}.$$

Since all conditions are met, a single break is sufficient to extinguish the arc effectively. However, to enhance device reliability, it is recommended to use two breaks. No additional components, such as arc chutes, shells, frames, or clamps, are required for this design.

6 THE CALCULATION OF SPRINGS

Electrical apparatuses commonly include one or more springs, which play a crucial role in defining the operational characteristics of these devices. Consequently, accurate spring calculations are essential.

Among various types, cylindrical helical springs are predominant, chosen based on the apparatus's kinematic design and mechanism construction.

Helical springs with substantial deflection are particularly suitable and find application in both small and large devices.

All calculations follow the methodologies outlined in [4].

6.1 Contact spring calculation

Given data for the calculation:

- P_p: Initial pullback force of the spring, equal to 11 N;
- f: Deflection, equal to 2.2 mm;
- G: Shear modulus, equal to 80000 N/mm^2;
- $\sigma_{p.st}$: Allowable torsional stress, equal to $580\ \mathrm{N/mm^2}$;
- c_n: Spring index, ranging from 4 to 10 for small spring wire diameters.

The diameter of spring wire:

$$d = \sqrt{\frac{8 \cdot P_p \cdot c_n}{\pi \cdot \sigma_{p.st}}}, \tag{6.1}$$

$$d = \sqrt{\frac{8 \cdot 11 \cdot 6}{\pi \cdot 580}} \approx 0.5384 = 0.6 \text{ mm}.$$

The spring diameter is determined by:

$$D = d \cdot c_n, \tag{6.2}$$

$$D = 0.6 \cdot 6 = 3.6 \text{ mm}.$$

The required number of turns is calculated using:

$$N = \frac{G \cdot d^4 \cdot 2 \cdot f}{8 \cdot D^3 \cdot P_p}, \tag{6.3}$$

$$N = \frac{80000 \cdot 0.6^4 \cdot 2 \cdot 2.2}{8 \cdot 11 \cdot 3.6^3} = 11.3169 \text{ turns}.$$

Rounding, the number of turns is taken as 12.

The actual bending f_a is:

$$f_a = \frac{8 \cdot D^3 \cdot P_p \cdot N}{G \cdot d^4}, \tag{6.4}$$

$$f_a = \frac{8 \cdot 3^3 \cdot 11 \cdot 12}{80000 \cdot 0.6^4} = 4.752 = 5 \text{ mm}.$$

Finally, the mechanical stress is checked as follows:

$$\sigma = \frac{16 \cdot P_p \cdot D}{2 \cdot \pi \cdot d^3}, \tag{6.5}$$

$$\sigma = \frac{16 \cdot 11 \cdot 3.6}{2 \cdot 3.14 \cdot 0.6^3} = 467 \ \frac{N}{mm^2},$$

$$\sigma \approx \sigma_{p.st},$$

$$467 \frac{N}{mm^2} < 580 \frac{N}{mm^2}.$$

The stress in the spring is within the permissible limit, confirming the design is suitable.

6.2 Opposing spring calculation

The initial data for the calculation:

- P_p: Final force of the pullback spring = 22 N;
- f: Deflection = 5 mm;
- G: Shear modulus = 80000 N/mm^2;
- $\sigma_{p.st}$: Allowable torsional stress = $580\ N/mm^2$;
- c_n: Spring index, typically ranging from 4 to 10 for small-diameter springs.

The diameter of spring wire:

$$d = \sqrt{\frac{8 \cdot P_p \cdot c_n}{\pi \cdot \sigma_{p.st}}}, \quad (6.6)$$

$$d = \sqrt{\frac{8 \cdot 22 \cdot 6}{3.14 \cdot 580}} \approx 0.7615 = 0.8 \text{ mm}.$$

The spring diameter is determined by:

$$D = d \cdot c_n, \quad (6.7)$$

$$D = 0.8 \cdot 6 = 4.8 \text{ mm}.$$

The required number of turns is calculated using:

$$N = \frac{G \cdot d^4 \cdot 2 \cdot f}{8 \cdot D^3 \cdot P_p}, \tag{6.8}$$

$$N = \frac{80000 \cdot 0.8^4 \cdot 2 \cdot 5}{8 \cdot 22 \cdot 4.8^{\,3}} = 16.835 \text{ turns}.$$

Rounding, the number of turns is taken as 17.

The actual bending f_a is:

$$f_a = \frac{8 \cdot D^3 \cdot P_p \cdot N}{G \cdot d^4}, \tag{6.9}$$

$$f_a = \frac{8 \cdot 4.8^{\,3} \cdot 22 \cdot 17}{80000 \cdot 0.8^{\,4}} = 10.098 = 10.1 \text{ mm}.$$

Finally, the mechanical stress is checked as follows:

$$\sigma = \frac{16 \cdot P_p \cdot D}{2 \cdot \pi \cdot d^3}, \tag{6.10}$$

$$\sigma = \frac{16 \cdot 22 \cdot 4.8}{2 \cdot 3.14 \cdot 0.8^3} = 525 \ \frac{N}{mm^2},$$

$$\sigma \approx \sigma_{p.st},$$

$$525 \frac{N}{mm^2} < 580 \frac{N}{mm^2}.$$

After performing these calculations with the appropriate values, the final results will confirm whether the opposing spring meets the required specifications.

Spring specifications:

- Material: carbon steel spring wire (ГОСТ 9389-75) for high-strength, cold-wound applications;
- Grade: I (B);
- Ultimate tensile strength: 2650 N/mm^2;
- Allowable torsional stress: 580 N/mm^2;
- Allowable bending stress: 930 N/mm^2;
- Shear modulus: 80000 N/mm^2;
- Elastic modulus: 200000 N/mm^2;
- Electrical resistivity: 0.19-0.22 $\cdot 10^{-6}$ Ohm· m.

7 MODELING IN THE FEMM PROGRAM

Finite Element Method Magnetics (FEMM) is a computer program used for solving low-frequency electromagnetic problems in 2D (two-dimensional) flat and axisymmetric areas. It uses the finite element method to study different types of electromagnetic fields. FEMM is very popular in electrical engineering and research because it is powerful, easy to use, and has strong computing abilities.

Why use an alternating current electromagnet in FEMM. Alternating current (AC) electromagnets are important parts in many devices, like transformers, electric motors, and inductors. Studying an AC electromagnet in FEMM helps engineers and researchers understand how magnetic fields behave with alternating current. That program is helpful for:

Optimizing Design: Making sure AC electromagnets are designed to work well and use energy efficiently. This means they can do their job without wasting too much energy.

Predicting Performance: Knowing how the electromagnet will work in different situations. For example, how strong the magnetic field will be at different times.

Minimizing Losses: Finding and reducing energy losses caused by things like eddy currents (small currents in the metal parts) and hysteresis (energy lost in the magnetic material).

Ensuring Safety: Making sure the electromagnet works safely within given limits. This means it will not get too hot or break under normal use.

Modeling the Electromagnet in FEMM:

Geometry Creation: First, draw the shape of the electromagnet using FEMM’s graphical interface. This includes the core, windings, and other parts. You use the mouse to draw and shape the parts on the screen.

Material Properties: Next, give the model the right material properties. FEMM has a large library of materials (like copper, iron, etc.), or you can add your own materials if needed. Each material has different properties like conductivity and permeability.

Boundary Conditions: Set the correct boundary conditions for the model. This means defining the electrical input (AC voltage or current), setting the frequency (how fast the current changes direction), and adding any external magnetic field conditions.

Mesh Generation: FEMM automatically divides the shape into small pieces (mesh). These small pieces help the computer calculate more accurately. You can change the mesh density to get the right balance between accuracy and computation speed. More pieces mean better accuracy but take longer to compute.

Calculating the Final Parameters:

After setting up the model, FEMM uses its solvers to do the calculations. For AC electromagnets, it solves the time-harmonic magnetic field equations. Important results include:

Magnetic Field Distribution: How the magnetic flux density (B-field) and magnetic field strength (H-field) are spread out in space. This shows where the magnetic field is strong or weak.

Inductance and Impedance: Values of inductance (how much the electromagnet can store energy in a magnetic field) and impedance (how much it resists the flow of AC current).

Eddy Current Losses: How eddy currents are distributed and their sizes in conductive materials. This shows where energy is lost as heat.

Force and Torque: Magnetic forces and torques (twisting forces) on the parts. This helps understand how the electromagnet moves or affects other parts.

Outputting the Final Picture of Magnetic Fields

When the calculations are done, FEMM offers several ways to see the results:

Field Plots: Colorful pictures showing the magnetic field distribution. These pictures show the size and direction of the fields, making it easy to see areas with high flux density. Red might show strong fields, while blue shows weak fields.

Vector Plots: Images that show the direction and size of the magnetic fields at different points in the model. Arrows can show which way the field points and how strong it is.

Contour Plots: Lines that show areas of constant magnetic potential or flux density, useful for detailed study. These lines help understand how the field changes in space.

Data Export: You can export numerical data for more analysis or to use in other software. FEMM supports exporting to different formats, like spreadsheets (Excel) and text files (TXT).

Reports: Detailed reports summarizing the analysis results, including important numbers, pictures, and calculation data. This can be printed or saved for future use.

Using FEMM to study AC electromagnets helps engineers and researchers understand the electromagnetic behavior of their designs, improving performance, efficiency, and safety. This means they can make better, safer, and more efficient electromagnets.

7.1 Description of the FEMM program

The magnetic preprocessor [16] is an essential tool for building the model's geometry, assigning material properties, and applying boundary conditions, all of which are foundational to setting up a magnetic analysis. This preprocessor provides a structured environment where users can visually construct and refine the geometric configuration of the problem before performing simulations. The geometry created in this preprocessor is composed of four primary types of elements:

Points define the start and end locations of linear and curved segments within the geometry. These points act as anchors, setting the locations where segments connect or terminate.

Connecting lines include both straight and curved segments that create the foundational structure of the geometry. Connecting lines bridge the points to form closed shapes or paths necessary for defining the problem space. These connections are critical for building complex contours and shapes, as well as for controlling current paths and field distributions.

Block labels are essential markers placed within specific regions of the geometry. These markers help assign material characteristics, such as magnetic permeability and

electrical conductivity, to defined areas. Additionally, they control the density and size of the computational mesh in each region, affecting the precision and computational efficiency of the solution.

Boundary conditions are specified along the external edges of the geometry to simulate real-world constraints or idealized limits. This can include setting boundaries that mimic open spaces, specific field intensities, or insulating edges, all of which impact the behavior of the magnetic fields within the problem space.

These elements collectively establish the setup and context for the magnetic analysis, ensuring that the geometric layout, material definitions, and boundary conditions are fully specified before running calculations.

The drawing preprocessor is the primary interface for creating and editing the geometry. Its core functionality includes multiple modes that enable users to build, organize, and modify objects with ease.

This point mode allows users to define precise points within the geometry. Points serve as reference nodes for connecting segments, providing exact locations where shapes begin or end.

In segment mode, straight line segments can be created between defined points. These segments form the backbone of linear elements in the geometry.

Arc segment mode is designed for creating curved segments, allowing users to add arcs and complex contours to the geometry. Curved segments are particularly useful in magnetic modeling where field behavior may be non-linear or involve rotational symmetry.

The block method allows users to assign material and physical properties to defined regions. By assigning these properties, users can simulate the behavior of different materials under magnetic fields, such as ferromagnetic, diamagnetic, or paramagnetic responses.

The group method is useful for managing and organizing multiple objects within the geometry. By grouping various elements, users can efficiently select, edit, and apply transformations or material properties to entire sets of objects at once, streamlining the setup process for large or complex models.

Together, these modes provide the flexibility needed to create detailed and accurate representations of magnetic systems. The combination of individual editing tools and organizational methods simplifies the process of constructing a model that aligns with real-world scenarios. After defining the geometry, the preprocessor provides a platform for refinement and verification, allowing users to make adjustments and ensure that the setup aligns with the intended physical parameters and boundary conditions before proceeding to solve the magnetic analysis.

To facilitate work in drawing mode, I used a grid object, which is represented by points marked across the drawing window surface. This grid provides a visual reference that helps align elements, ensures precision in placing points and segments, and assists in maintaining proportionality within the geometry. The grid simplifies the layout process, making it easier to position and connect elements accurately, especially in complex configurations or when symmetry is needed.

In the program, objects are selected by drawing a rectangular or circular selection frame while holding down the left mouse button. This will select only the objects that are currently active, such as points, lines, arcs, or blocks. Using the commands in this menu, I can copy any selected object to the clipboard, delete it, move or rotate it, scale, mirror, or round it. These tools provide flexible options for editing and transforming objects, allowing for precise customization and efficient refinement of the geometry.

I specify the exact coordinates for each point. This can be done in either Cartesian coordinates (x, y) for planar positioning or cylindrical coordinates (r, θ) if working in a rotational framework. Accurate point placement is critical, as it ensures that all subsequent lines and segments align precisely according to the design requirements.

To create straight lines between points, I switch to Line Drawing Mode. In this mode, I can draw linear segments by connecting predefined points, forming the main structure and edges of the geometry. These lines define the boundary and internal structure of the model, serving as the framework for regions with specific properties or behaviors.

For drawing arc segments, I activate Segment Drawing Mode, allowing me to create curved paths essential for rounded or complex contours. In the dialog box, I enter several key parameters:

Arc angle – defines the curvature of the arc.

Maximum discretization angle – sets the level of detail for the arc by controlling the angle of each subdivided segment.

Boundary conditions – conditions may be applied if required, such as magnetic insulation or specific field values.

The direction of the arc's curvature depends on the order of selected points, with the positive contour direction determining the arc's convexity. This feature enables flexibility in designing structures with non-linear or circular properties, as often required in electromagnetic modeling.

To prepare the model for analysis, I follow these steps to define the problem parameters:

I select a 2D analysis type to simplify the model and reduce computational load, ideal for planar or axisymmetric problems.

I specify the units for measurements in the drawing window, such as meters, centimeters, millimeters, or inches. Consistent unit selection is essential for ensuring that all parameters align correctly during simulations.

Since I am working with a permanent magnet and require a static field analysis, I set the frequency to Hz = 0. This setting is crucial for simulating scenarios without alternating currents or time-varying fields.

For 2D models, the depth parameter represents the extent of the model along the z-axis. This depth value is important when extrapolating 2D results to three-dimensional interpretations, especially in cases with uniform fields along the z-axis.

I set the accuracy of the iterative solver to a high precision level (e.g., up to 1×10^{-16}). This precision ensures reliable results, particularly for complex or high-field-intensity scenarios.

To control the quality of the mesh in complex regions, I define a minimum angle for triangular elements. Reducing this angle may help capture finer details in intricate

geometries, but caution is needed as excessively small angles can lower solution accuracy in high-gradient areas.

I can add comments within the project to record important details, assumptions, or unique setup notes. These comments serve as a reference, ensuring all relevant information is available when revisiting or sharing the project.

This structured approach ensures that each aspect of the model is carefully configured for accurate, efficient simulation, ready for subsequent analysis and interpretation.

To solve the problem, I need to define boundary conditions, materials, and block properties. Depending on the type of problem being solved, real or imaginary values can be entered for property values. By setting the frequency to zero, I can enter quantities with a complex part equal to zero:

$$\overrightarrow{\{A\}} = A_{\{re\}} \cdot cos(\omega \cdot t) + i \cdot A_{\{im\}} \cdot sin(\omega \cdot t)$$

I need to set boundary conditions for accurate and correct problem-solving. These conditions define how the system behaves at its boundaries and are necessary for proper simulation of physical phenomena. Each time I add or modify an existing boundary condition, a dialog box opens for configuration. To ensure easy identification, I need to assign each boundary a unique name.

Different types of boundary conditions I will use:

Prescribed magnetic potential:

This is the main boundary condition set by default. It allows me to specify the magnetic potential along the boundary. For example, if I need to simulate magnetic flux that runs parallel to the object's boundary, I will use this condition. Specifically, if I want to set magnetic insulation, I set the potential value to A = 0. I can configure this boundary condition by setting parameters A0, A1, A2, and phase, which is especially useful for 2D or axisymmetric problems where it's important to control the distribution of the magnetic field. In this case, for a planar or axisymmetric problem:

$$A = (A_0 + A_1 \cdot x + A_2 \cdot y) \cdot e^{\{i\,\varphi\}}$$
$$A = (A_0 + A_1 \cdot r + A_2 \cdot z) \cdot e^{\{i\,\varphi\}}$$

Thin layer (Small Skin Depth):

I will use this condition for cases where there is a pronounced surface effect and eddy currents are concentrated in a thin surface layer. This is necessary in high-frequency fields where the penetration depth of the current becomes minimal. By applying Robin conditions with complex coefficients, I account for the conductivity and permeability of the layer, which yields a more accurate solution for such problems.

Mixed Condition $\frac{1}{\mu_0 \cdot \mu_r} \cdot \frac{\partial A}{\partial n} + c_0 \cdot A + c_1 = 0$:

This condition is useful in two cases:

If I want to simulate an infinite space (an open boundary), I will choose the coefficient c0 with c1=0 at the outer boundary. This helps reduce the impact of the surrounding environment in the simulation.

If I need to specify a certain value of the magnetic field along the boundary, I will set c0=0 and c1=H (where H is the magnetic field strength in A/m). The default condition can be used for cases requiring a flow of magnetic field perpendicular to the boundary, enhancing modeling versatility $\frac{\partial A}{\partial n} = 0$.

Strategic dual image:

I will use this condition when I need to simulate external boundaries in a two-dimensional problem. It is especially useful when it’s necessary to simulate an infinite space for a constant magnetic field. I will apply this condition only to the outer boundaries, where the relative magnetic permeability is 1 and where there are no currents.

Periodic boundary:

This condition allows me to set the same magnetic potential value on two boundaries. It will be useful when I want to reduce the modeling area, describing open

boundaries in this way. This reduces computational resource demands since a smaller area will need to be modeled.

Anti-periodic condition:

This condition, like the periodic condition, applies to a pair of boundaries, but the difference is that the magnetic potential value on one boundary is the opposite of that on the other. I will use this condition when I need to reduce the modeling area, for example, when considering a part of an electric machine.

Material Properties:

The "Material Properties" section is essential for defining the material characteristics of the object associated with the block label in the simulation model. This section allows me to specify various attributes of the material, ensuring that each region in the model accurately reflects its physical characteristics and behavior under different electromagnetic conditions. By carefully setting these properties, I can achieve a more realistic and accurate simulation that aligns with the actual performance of the materials in real-world applications. When creating a material, I first need to perform a series of actions: assign a unique name to the material, which serves as an identifier, allowing me to easily reference it and distinguish it from other materials; determine whether the B-H (magnetic flux density versus magnetic field strength) relationship will be linear or nonlinear, which is critical as it affects how the material responds to applied magnetic fields; specify anisotropic values of μ_r, (relative permeability) for materials with a linear B-H relationship, especially important for materials exhibiting directional properties; and set the angle of lag of the hysteresis curve for harmonic problems where hysteresis creates a constant phase lag between B and H that is independent of frequency. This approach is effective under the assumption that the hysteresis loop has an elliptical shape, but since the loop is not perfectly elliptical, the angle needs to be adjusted based on the amplitude of the input signal. The lag angle is a crucial parameter for sintered steel, typically ranging from 0 to 20 degrees, influencing the material's response to varying magnetic fields. In the case of a nonlinear B-H relationship, I must input the corresponding data points manually. By pressing a designated key, I can enter specific values that describe the material's behavior under nonlinear conditions, which is critical for capturing the

complexities of how the material reacts to varying magnetic fields. Once the data is entered, I can observe the resulting curve on a graph. The program employs spline smoothing to enhance the visual representation of the data, and in some cases, to obtain a smoother curve, I may need to either increase the number of input points or adjust the existing data points. This iterative process helps refine the accuracy of the representation. If the calculated values exceed the data range, particularly during instances of high saturation, the program automatically extrapolates the data, extending the series beyond the original input. This feature is useful for simulating conditions that may exceed the standard operating parameters of the material. The program includes a window that allows me to account for the lag angle during hysteresis for nonlinear problems, where it is assumed that the lag angle is proportional to the effective magnetic permeability. The highest magnetic permeability is taken as the maximum permeability:

$$\varphi_h(B) = \left(\frac{\mu_{eff}(B)}{\mu_{eff,max}}\right)\varphi_{h,max}$$

By meticulously defining these material properties and their relationships, I can create a robust model that accurately simulates the behavior of the material under various electromagnetic conditions, leading to reliable and meaningful results in my analysis.

By specifying the properties μ_r and H_c, I define materials for a permanent magnet. The window also allows me to set the density of external source currents in the block when using direct current. I can also set the density of external source currents in the block when using direct current. However, it is recommended to use the "current properties" to define the total current in the object. Additionally, I can specify the material's conductivity in MS/m.

The final property allows me to set the lamination of the material and the type of wire. The flux is continuous if it flows along the lamination and experiences interruptions if it flows across it, figure 7.1 shows examples of flux passing through laminated material.

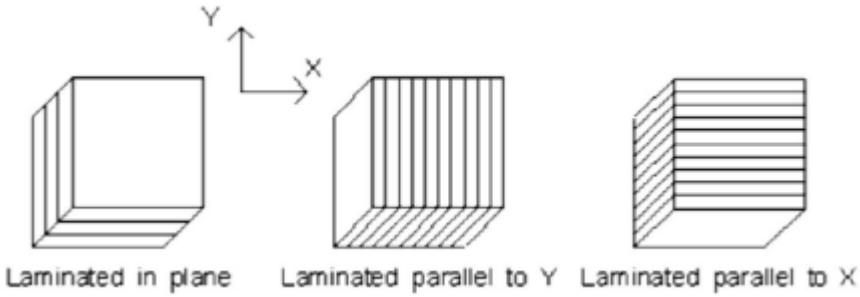

Figure 7.1 – Examples of flux passing through lamination

Special Attributes:

In the "Special Attributes" section, I can define key parameters that influence how the material behaves under electromagnetic conditions. This section lets me select the flux direction, the lamination thickness, and the fill factor. These values are especially important when modeling materials with complex behaviors, as they help account for both hysteresis and eddy currents in harmonic problems, enabling more accurate simulations in dynamic electromagnetic fields. For magnetostatic scenarios, this setup allows for capturing the effects of nonlinear lamination without needing to model each lamination layer individually.

If the material is homogeneous, I leave the "Lamination Thickness" field at 0, as no layering is present. Otherwise, I enter the thickness of the iron sheet in millimeters, representing the distance of each lamination layer. Next is the fill factor, which defines the portion of the core filled with iron as a decimal. For instance, a fill factor of 0.9 means that 90% of the core space is occupied by iron. This factor directly impacts the material's magnetic performance by controlling how densely the core material is packed, affecting how efficiently magnetic flux flows through the material.

When choosing the wire type, additional diameter fields become available for detailed customization. For stranded and spiral wires, I can specify both the diameter of each strand and the total number of turns. This feature is crucial in modeling complex wire geometries where multiple strands or coils are present. For square and magnet wires, only a single conductor is implied, simplifying the configuration. Starting with the "magnet wire" option, I can set a linear B-H relationship with the option of anisotropy,

which applies directionally dependent properties. This is particularly useful for applications where the magnetic properties vary along different axes.

Specifying the wire type also means that the material property can apply to the entire space occupied by the wire, removing the need to model each individual conductor in detail. For direct current (DC) conditions, the program automatically adjusts the results based on the fill factor, which ensures accuracy by accounting for the wire's space usage within the material.

For magnet wire, which is available when the B-H relationship is linear and magnetic permeability is constant, I can define the wire diameter directly, affecting how current flows through the conductor.

Circuit Property

Here, I specify the current flowing through the magnet. First, I need to assign a name to the current for easy identification in the model later on. Then, I set the current strength which in my case is 110 amperes, which is critically important for accurately modeling the magnetic field generated by the current.

Correctly setting these parameters is essential for ensuring the accuracy and reliability of calculations in the electromagnetic model.

Properties of the Selected Block

Here, I specify the materials from which the electromagnet is made, the number of turns in the coil, and select the circuit that I created earlier. Defining the materials is essential because different materials will affect the magnetic properties and overall efficiency of the electromagnet.

Additionally, by selecting the appropriate circuit, I can ensure that the electromagnet integrates effectively with the rest of the electrical system, allowing for optimal performance in its intended application. This careful configuration is vital for achieving the desired electromagnetic characteristics and functionality.

7.2 Building a model of an DC electromagnet

After completing all the necessary steps, I created a model of a DC electromagnet, which we can see in figure 7.2 that includes several key elements: a stainless steel core, an air gap, and a winding [16].

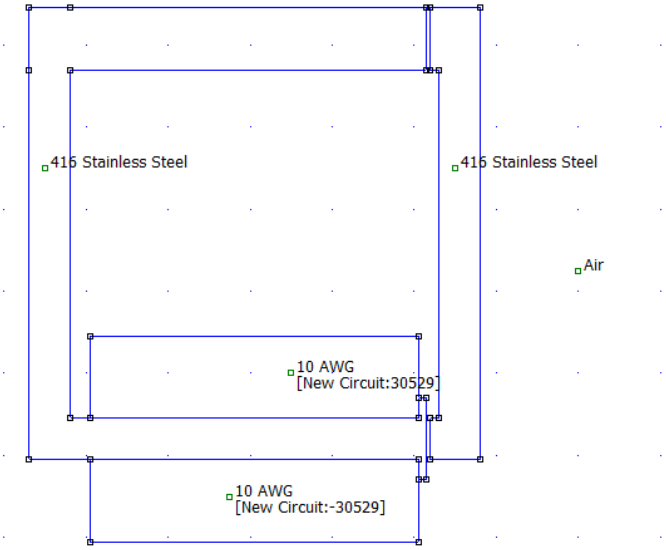

Figure 7.2 – The model of an DC electromagnet

I defined two rectangular sections made of 415-grade stainless steel, which form the magnetic core of the electromagnet. This material was chosen to control the magnetic flux and ensure the durability of the structure.

In the model, I also included an air gap, labeled as "Air." The air gap is essential for controlling the path of the magnetic flux and for storing magnetic energy.

For the winding, I used 10 AWG wire and added a coil with 30529 turns. Each coil carries a current of 110 amps, which generates a strong magnetic field required for the electromagnet’s operation.

This model allows me to analyze the distribution and behavior of the magnetic field within the electromagnet, including parameters such as flux density, field intensity, the attraction force on the plate, and potential losses in the air gap.

Figure 7.3 shows the same model of the DC electromagnet, with a visualization of the magnetic flux density distribution, allowing for a detailed analysis of the magnetic field behavior. We can observe how the magnetic field lines pass through the stainless steel core, concentrate around the coil, and close within the air gap. These magnetic flux lines follow the path of least resistance, forming closed loops and showing the path of the flux through different materials in the model.

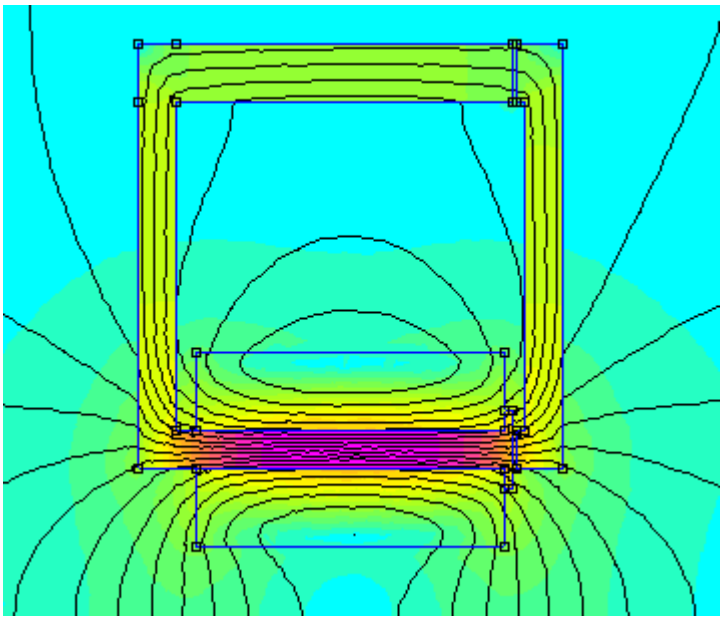

Figure 7.3 – Flux density (T)

The highest density of lines is seen around the coil, where the energy of the magnetic field is concentrated. This corresponds to areas of the highest magnetic flux density, as the primary magnetic field of the electromagnet is generated here.

The color gradients displayed in the image vividly depict the change in magnetic flux density: more saturated colors, such as purple and red, indicate high flux density in the coil area where strong currents generate a powerful magnetic field. Zones with green and blue shades represent areas with lower flux density, showing the weakening of the magnetic field as it spreads away from the source — the coil.

This visualization not only facilitates the analysis of the distribution and intensity of the magnetic field but also shows how materials with different magnetic properties interact. It helps identify areas of highest and lowest flux density, potential areas of flux

loss in the air gap, and enables adjustments to the model's parameters to optimize the electromagnet's performance.

7.3 Results of the software analysis

In this section, I will present the types and results of the studies that can be conducted in the program [16].

Results of the point analysis:

In the figure 7.4 I put a point from which I took the following results:

1.Coordinates of the point x=4.55 and y=3.68: These values indicate the location of the point in two-dimensional space. In FEMM, this is necessary for defining the position of the area being analyzed in the magnetic or electric field.

2. Magnetic Flux A = 0.0802818 Wb/m : This value indicates the amount of magnetic flux passing through a unit area. It can be used to calculate the magnetic characteristics of systems such as transformers or electric motors. An important aspect: the larger the value, the greater the magnetic flux.

3. Magnetic Field Density |B| = 2.17949 T: This value indicates how strong the magnetic field is at the given point. The magnetic field density is important for understanding how charged particles or conductors will behave in this field. It is also crucial for estimating the force acting on a conductor with current placed in a magnetic field.

4. Components of the Magnetic Field Bx = 1.30459 T: This is the component of the magnetic field along the x-axis. It shows how the magnetic field influences this axis. By = 1.74592 T: This is the component of the magnetic field along the y-axis. Similarly, it shows the influence of the magnetic field along the y-axis.

5. Magnetic Field Intensity |H| = 392369 A/m: The intensity of the magnetic field is a measure of the magnetic force applied per unit length. It helps understand how the field will affect magnetic materials and charged particles.

6. Components of the Magnetic Field Hx = 234862 A/m: This is the component of the magnetic field intensity along the x-axis. This value may be useful for calculating the

force acting on magnetic materials in this area. Hy = 314314 A/m: This is the component of the magnetic field intensity along the y-axis. It allows for determining how the magnetic field influences this axis.

7. Permeability μx= 4.42028 (relative) and μy= 4.42028 (rel) (relative): These values indicate how well materials conduct magnetic lines in the corresponding directions. The relative permeability compares the permeability of the material to the permeability of vacuum (where $\mu_0 = 4\pi \cdot 10^{-7}\,\mathrm{H/m}$). The higher the relative permeability, the better the material conducts magnetic lines.

8. Energy of the Magnetic Field E = 106271 J/m^3: This is the energy stored in the magnetic field per unit volume. It can be useful for estimating energy losses in electrical devices or for designing magnetic systems.

9. Current Density J = 0 MA/m^2: The density of electric current at this point is zero, which may indicate the absence of electric current in this area or that this point is in an inactive zone concerning the electric field.

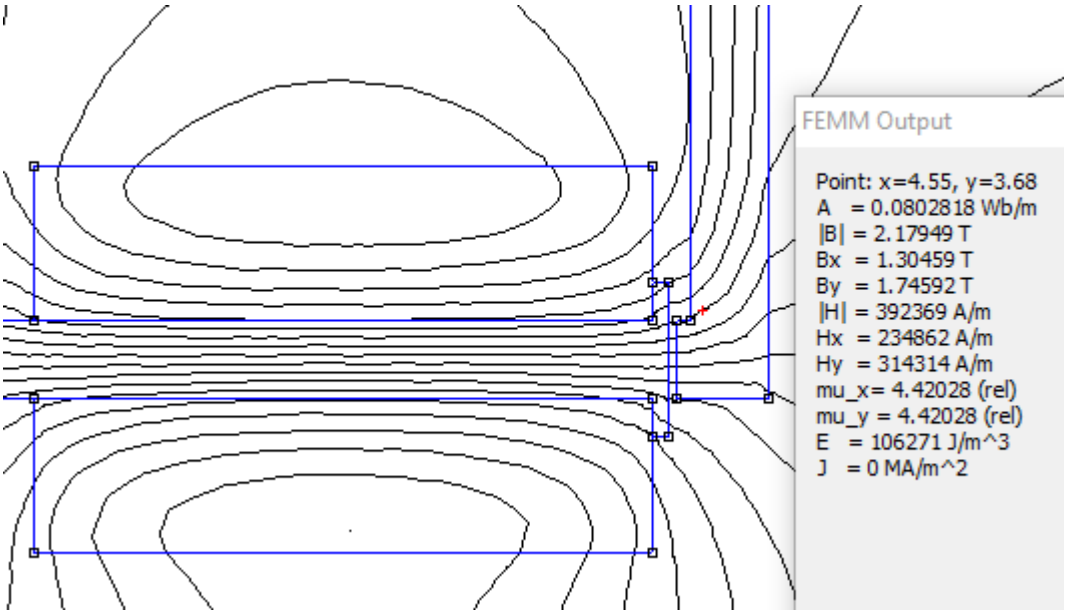

Figure 7.4 – Mode Point

Results of integration along the line:

If I choose a contour like in figure 7.5, I can calculate linear integrals along the contour. In the case of a harmonic problem, the integral is calculated in the form of a

complex number. Line integrals play a key role in the analysis of electromagnetic fields, allowing for the evaluation of various physical quantities along a given path. These integrals can be used to solve numerous problems related to magnetic and electric fields, including the assessment of flux and forces acting on conductors.

Types of Integrals: Bn – This integral returns the flux normal to the contour, as well as the average value of the flux density. It allows us to assess how much magnetic flux passes through the chosen contour, which is important for understanding the interaction of the magnetic field with surrounding objects.

$$\text{Normal Flux} = 7.99292 \cdot 10^{-6}\ \text{Webers}$$
$$\text{Average B} \cdot \text{n} = 0.00225255\ \text{Tesla}$$

$H\tau$ – This integral returns the field intensity between the endpoints of the contour. It is used to determine the influence of the magnetic field on conductors located along this contour and can aid in analyzing the electrical characteristics of the system.

$$\text{MMF Drop Along Contour} = 278538\ \text{Amp-turns}$$
$$\text{Average } H \cdot t = 1.99383 \cdot 10^{6}\ \text{Amp/Meter}$$

Contour Length – This calculates the length of the contour in meters. This parameter is necessary for determining the characteristics of magnetic and electric fields, as the contour length affects the field distribution and the magnitude of the integrals.

$$\text{Contour Length} = 0.11\ \text{meters}$$
$$\text{Surface Area} = 0.00354839\ \text{m}^2$$

Force Tensor – This integral calculates the force acting on the contour according to Maxwell's tensor. The force acting on the contour can be used to assess the interaction

between magnetic fields and conductors, which has practical applications in devices such as electric motors and transformers.

$$\text{Force in } x\text{-direction} = 24.3214\,\text{N}$$
$$\text{Force in } y\text{-direction} = -16624.2\,\text{N}$$

Torque Tensor – This integral calculates the moment about the axis (0, 0) acting on the contour. This value helps determine how external magnetic and electric fields may cause rotation of conductors or magnetic objects, which is also important in a number of engineering applications.

$$\text{Torque about } (0,0) = -866.205\,\text{N}\cdot\text{m}$$

$Bn2$ – This integral represents the integral of the square of the induction. It allows for the assessment of magnetic field distribution along the contour and can be used to analyze energy losses in systems where high values of magnetic induction may cause significant energy losses.

$$\text{Result} = 0.00772401\,\text{Webers}^2$$
$$\text{Average } (Bn)^2 = 0.0552899\,\text{Tesla}^2$$

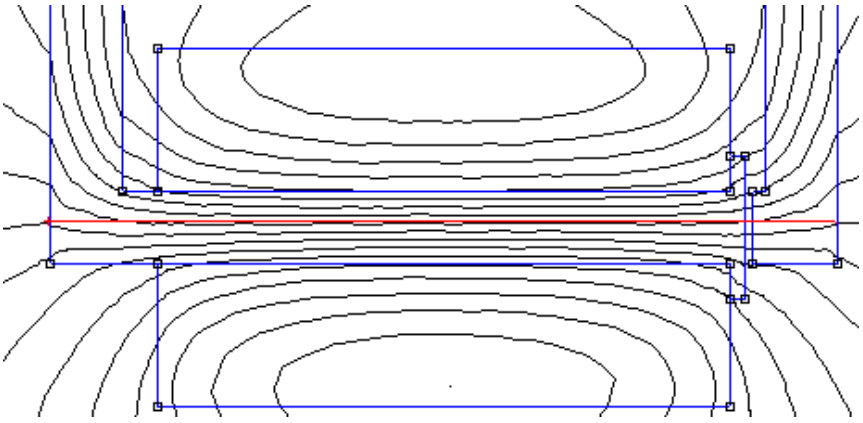

Figure 7.5 – Contour

Results of integration over the specified area:

If a specific area is chosen like in figure 7.6, a series of integrations can be performed over it.

1. JA integral:

The JA integral is defined by the following expression:

$$JA = \int_V dV \cdot J_A \, [\text{Гн} \cdot \text{А}^2]$$

This integral allows the calculation of the self-inductance L of the region with a known current i:

$$L = \left(\frac{1}{2}\right) \cdot \int_V J_A \cdot dV$$

This calculation applies only to linear problems where the inductance remains constant.

Result of the software calculation:

$$995.212 \, \text{Гн} \cdot \text{А}^2$$

2. A integral:

The A integral is calculated using the formula:

$$A = \int_V dV \cdot A \, [\text{Гн} \cdot \text{А} \cdot \text{м}^2]$$

This integral can be used to calculate the mutual inductance M, defined as:

$$M = \left(\frac{1}{2}\right) \cdot \int_{V_2} J_2 \cdot A_1 \cdot dV$$

where A1 is the magnetic potential from the first loop intersecting the second, J2J is the current density of the second loop, and V2 is the volume of the second loop. By using the relation $S = J \cdot i$, the current density can be expressed through the values of current, turns, and area:

$$M = \int_{V_2} (J_2 - J_1) \cdot A \cdot dV$$

Calculation of M is simpler when both loops carry the same unit current, as the inductance of linear systems is independent of current. For harmonic problems, the values of mutual inductance M will be complex and vary with frequency. The second part of the A integral (H·A) gives the flux, adjusted by flux linkage. To obtain the complete flux linkage, this value should be multiplied by the number of turns in the loop.

Result of the software calculation:

Integral of A over the selected area:

$$\int AdV = 7.65008 \times 10 - 6\ Henry \cdot Amp \cdot meter^2$$

Integral of A per selected area:

$$\frac{\int A\ dV}{\text{selected area}} = 0.00296441\ \text{Henry} \cdot \text{Amp}$$

3. Magnetic field energy:

This option can be used as an alternative way to calculate inductance in linear or unsaturated systems. Inductance is defined by the formula:

$$E = \left(\frac{1}{2}\right) \cdot L \cdot i^2$$

For nonlinear materials, the energy is calculated by the formula:

$$E = \int_V B \cdot H \cdot dV$$

Result of the software calculation:

77.0188 Joules

4. Magnetic co energy:

Co energy is calculated by the formula:

$$W = \int_V H \cdot B \cdot dV$$

For nonlinear problems. This method is used as an alternative for calculating force or torque. The force or torque is given by:

$$M = \frac{W(q + dq) - W(q)}{dq}$$

where q is the coordinate along which the force is calculated, and dq is the coordinate increment.

Result of the software calculation:

77.0188 Joules

5. Hyst. and (or) laminated eddy current losses:

Used to determine losses in laminated steel stacks in harmonic problems.

Result of the software calculation:

0 Watts

6. Resistive losses:

The integral calculates the value of i^2R in the direction perpendicular to the cross-sectional plane (z or φ) if the material's conductivity is specified.

Result of the software calculation:

3072.52 Watts

7. Block cross-section area:

Calculates the cross-sectional area.

Result of the software calculation:

$0.00258064\ \text{meter}^2$

8. Total losses:

Calculates total losses in the selected area. If a loss angle is specified for steel, both resistive (Ohmic) and hysteresis losses are calculated.

Result of the software calculation:

3072.52 Watts

9. Lorentz force (J·B):

This integral calculates the Lorentz force by the formula:

$$F = \int_V J \times B \cdot dV$$

Result of the software calculation:

x-component: 19.7059 N

y-component: 11086.6 N

10. Lorentz torque (r·J·B)

Determines the torque due to the Lorentz force acting on a current-carrying conductor in a magnetic field.

Result of the software calculation:

Torque about (0,0): 575.925 N*m

11. B Integral across the block:

Can be used to calculate Lorentz forces or average induction across a volume.

Result of the software calculation:

x-component: 8.52213e-005 Tesla meter^3

y-component: -1.51477e-007 Tesla meter^3

12. Total current:

Calculates the current across the selected section, useful for assessing current distribution in conductors.

Result of the software calculation:

335720 Amps

13. Block volume:

Determines the volume of the block, required for various calculations.

Result of the software calculation:

$6.55483e\text{-}005\ meter^3$

14. Torque via Weighted Stress Tensor:

Calculates torque based on the Maxwell tensor relative to an axis at coordinates (0, 0).

Result of the software calculation:

Torque about (0,0): 483.257 N*m

15. Moment of Inertia (R^2):

Calculates the moment of inertia relative to the Z-axis (x = 0, y = 0), and for axisymmetric problems, relative to the axis r = 0. For the final result, this integral must be multiplied by the material's density.

Result of the software calculation:

$$\text{Integral of}(x^2 + y^2): 8.97445 \times 10^{-7}\ m^5$$

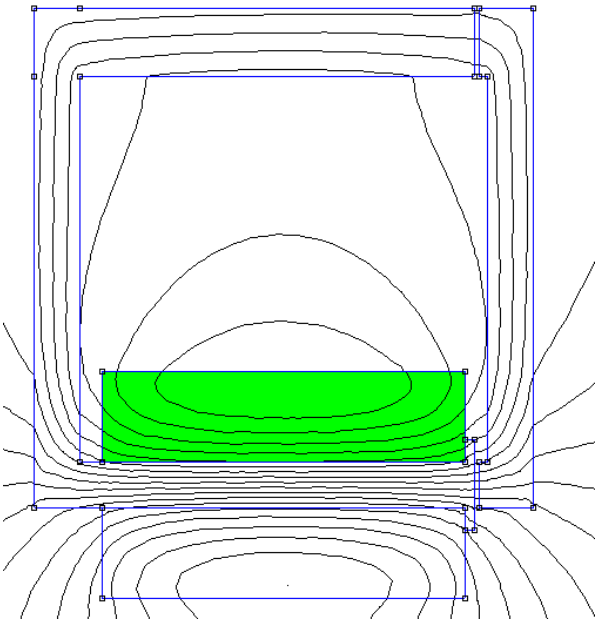

Figure 7.6 – Chosen area

16. Force via weighted stress tensor:

We can calculate the force through the weighted stress tensor only via the adjacent plate, as shown in figure 7.7. Determines forces acting on an object according to the Maxwell tensor. The program selects an integration path to yield the best result by solving the Laplace equation.

Result of the software calculation:

x-component: -1332.54 N

y-component: -281.982 N

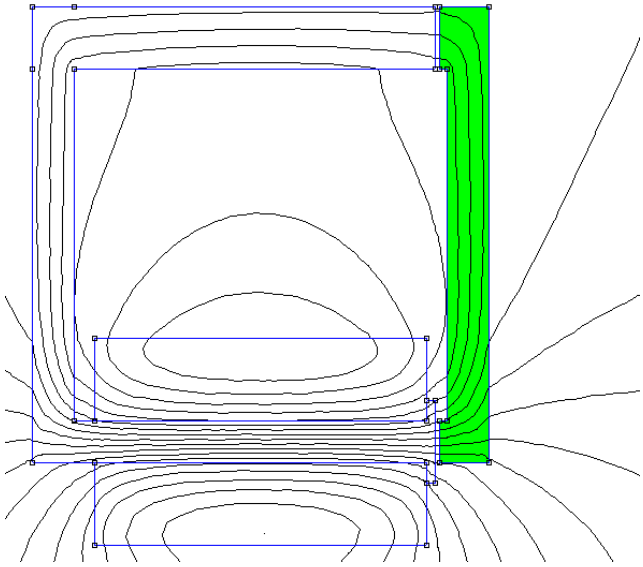

Figure 7.7 – The plate that is attracted by the magnetic field.

Circuit properties:

We can view the circuit parameters in the program:

Parameter	Value
Total current	110 Amps
Voltage Drop	55.8641 Volts
Flux Linkage	8.49869 Webers
Flux/Current	0.0772608 Henries
Voltage/Current	0.507855 Ohms

Power	6145.05 Watts

Plots of the field values:

To plot the dependency graphs, I first need to draw a line as shown in figure 7.8.

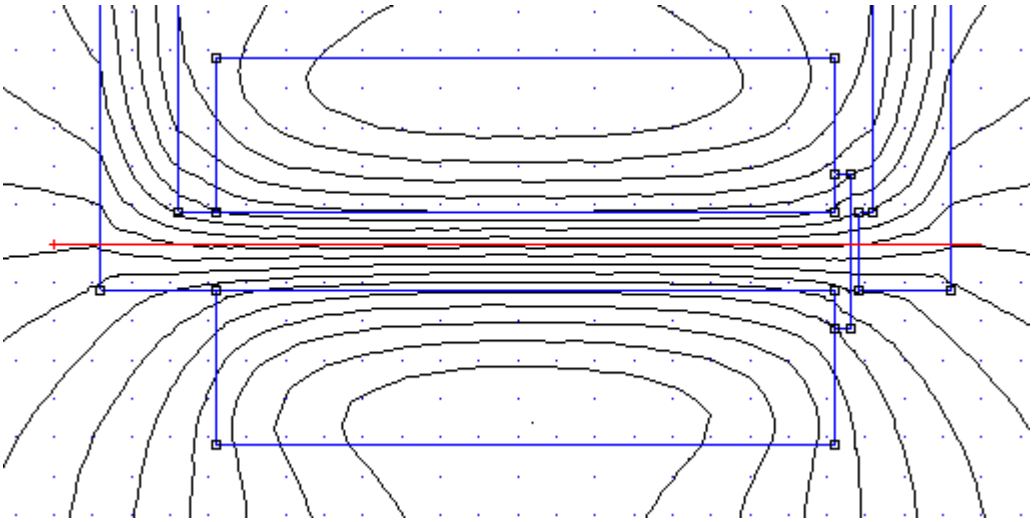

Figure 7.8 – Measuring line

After that I can start exploring the plots. The first plot on the figure 7.8 illustrates the variation of magnetic potential along the length of an electromagnet. The horizontal axis represents the length in inches, and the vertical axis shows the magnetic potential in Webers per meter (Wb/m). The shape of the curve provides insight into the magnetic field distribution within the electromagnet.

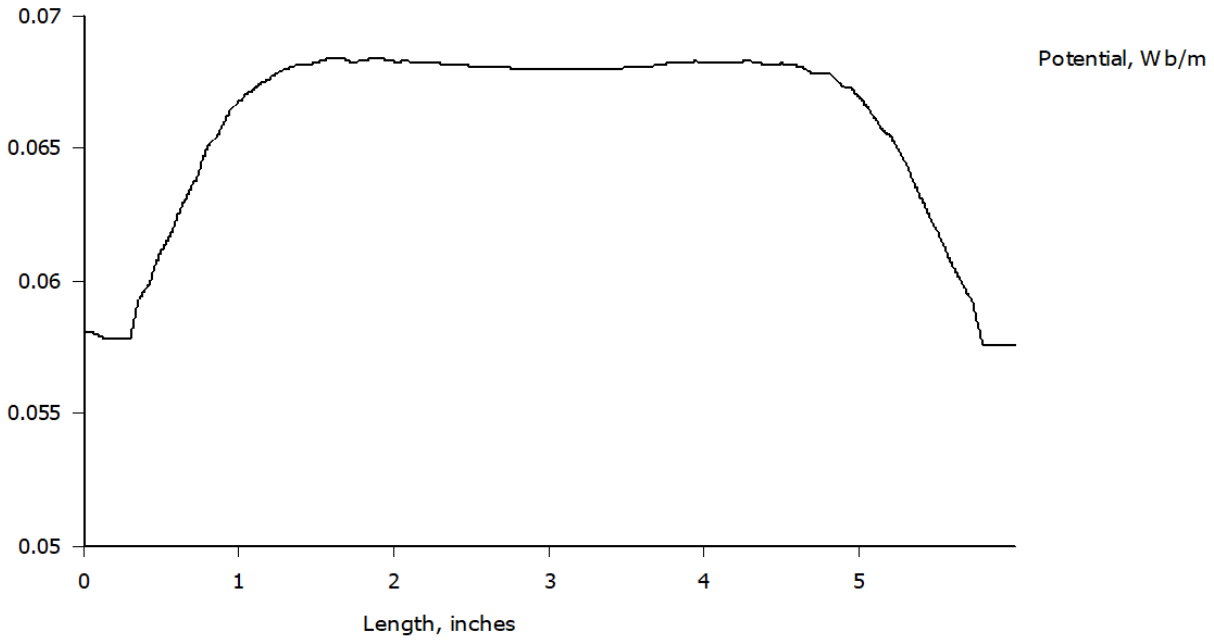

Figure 7.8 – Potential plot

Analysis of the curve:

Initial low potential Region (0 to ~0.5 inches):

At the leftmost edge of the graph, the magnetic potential begins around 0.052 Wb/m. This low initial value suggests that this part of the electromagnet has minimal magnetic field concentration.

There is a small but noticeable increase in potential as the length progresses, indicating that the magnetic field begins to strengthen within the first half-inch.

Sharp increase region (~0.5 to ~1 inch):

Between 0.5 and 1 inch, the curve shows a steep rise in magnetic potential, reaching approximately 0.065 Wb/m.

This sharp increase suggests a rapid buildup of the magnetic field, likely as the field lines concentrate towards the core of the electromagnet.

Plateau region (~1 to ~5 inches):

From about 1 inch to 5 inches, the magnetic potential remains almost constant, creating a plateau at around 0.065–0.067 Wb/m.

This flat section represents a stable and uniform magnetic field within this central region, likely corresponding to the core or main body of the electromagnet. The relatively

consistent magnetic potential here indicates that the field is well-distributed in this area, which is typically desired for an effective magnetic field.

Gradual decline region (~5 to ~6 inches):

After 5 inches, the magnetic potential starts to decrease gradually until it returns to approximately 0.052 Wb/m near the 6-inch mark.

This tapering off suggests that the magnetic field weakens as it approaches the end of the electromagnet. This decline in magnetic potential is consistent with the typical behavior of magnetic fields, which tend to spread out and weaken near the edges or boundaries.

End region (after ~6 inches):

The curve levels off near 0.052 Wb/m, similar to the initial value at the starting point of the graph, suggesting a symmetry in magnetic field distribution along the length of the electromagnet.

Summary: The graph highlights a strong, uniform magnetic field in the central region of the electromagnet (1 to 5 inches), with weaker fields at the edges. This distribution indicates that the electromagnet is likely designed to concentrate the magnetic field within its core, with the ends contributing minimally to the overall field strength. This is a typical profile for a well-designed electromagnet, where the core area provides the primary magnetic effect.

The figure 7.9 displays the variation of magnetic flux density, represented by |B|, in Teslas along the length of an electromagnet. The x-axis shows the length in inches, while the y-axis indicates the magnetic flux density in Teslas.

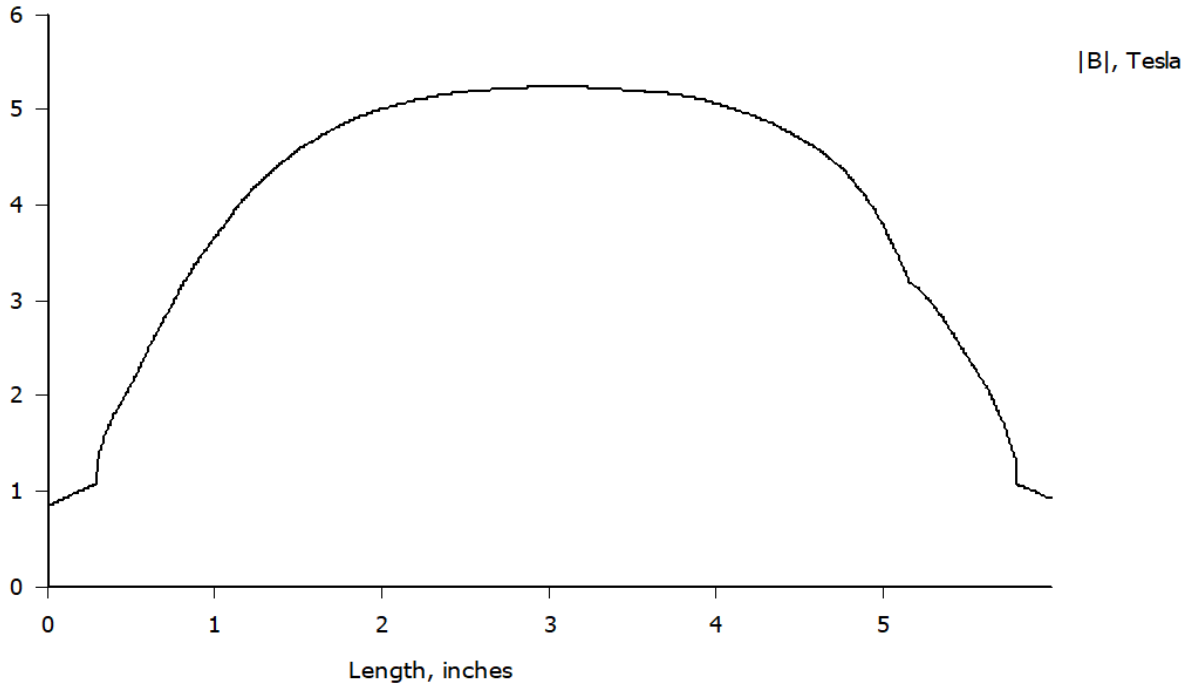

Figure 7.9 – Magnitude of the flux density

Analysis of the Curve:

Initial low flux density region (0 to ~0.5 inches):

At the left edge of the graph, the magnetic flux density begins at approximately 1 Tesla. This relatively low starting value suggests that the magnetic field strength is minimal at the edge of the electromagnet.

As we move from 0 to around 0.5 inches, there is a sharp increase in |B|, indicating the field is rapidly intensifying.

Rapid Increase Region (~0.5 to ~1.5 inches):

Between 0.5 and 1.5 inches, the magnetic flux density rises sharply, reaching nearly 5 Teslas.

This increase reflects a high concentration of the magnetic field as the flux density builds up towards the core of the electromagnet.

Plateau region (~1.5 to ~4.5 inches):

From about 1.5 inches to 4.5 inches, the magnetic flux density remains almost constant at a peak value around 5 Teslas, creating a plateau in the graph.

This flat portion signifies a stable, uniform magnetic field distribution in the central region of the electromagnet. This high and consistent field strength is likely by design, where the electromagnet core generates a strong, uniform magnetic field.

Gradual decline region (~4.5 to ~6 inches):

After 4.5 inches, the magnetic flux density begins to decrease, gradually tapering off to around 1 Tesla by the 6-inch mark.

This reduction reflects the weakening of the magnetic field towards the end of the electromagnet, consistent with field distribution that naturally weakens near the edges.

Symmetry of the curve:

The curve is nearly symmetrical about the center of the plateau, which indicates an even distribution of magnetic flux density along the length of the electromagnet's core. This symmetry suggests a balanced design, where both ends of the electromagnet have similar field strengths.

Summary: The graph shows that the electromagnet has a strong and uniform magnetic flux density in its central region (1.5 to 4.5 inches), with weaker fields towards the edges. The central peak reaching 5 Teslas signifies the core's role in generating a strong magnetic field, while the edges have minimal impact on the overall field strength.

The figure 7.10 shows the dependence of the normal component of magnetic induction Bn, expressed in teslas (Tesla), on the length in inches.

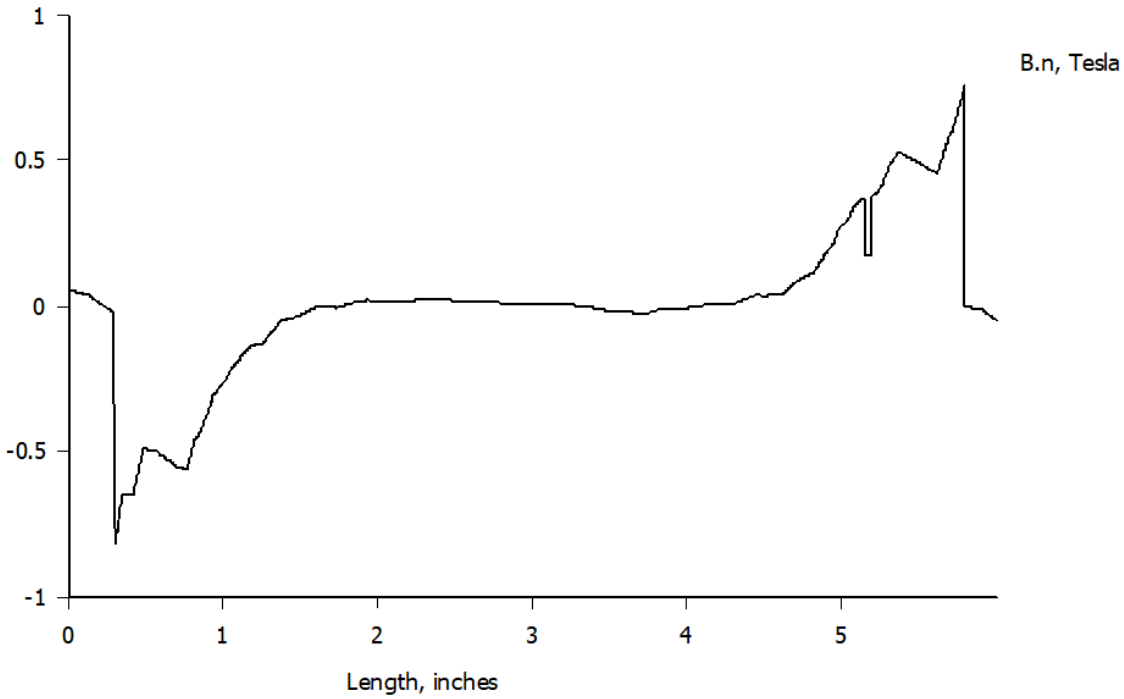

Figure 7.10 – Normal flux density

Graph Description:

Initial section (from 0 to ~1 inch): There is a sharp drop in the normal component of magnetic induction to around -0.5 T. This indicates an area where the flux direction is opposite to the main field orientation.

Middle section (from ~1 to ~4 inches): The flux density remains relatively stable around zero, indicating minimal normal magnetic flux component in this region.

Final section (from ~4 to ~6 inches): The graph rises, with Bn increasing to approximately 0.6 T, along with some fluctuations and sharp peaks. This may suggest the presence of a strong magnetic field in this region and inhomogeneities in the magnetic flux distribution.

The graph illustrates a variable magnetic flux density along the length, with distinct changes in the initial and final regions.

The figure 7.11 displays the dependence of the tangential component of magnetic induction Bt, measured in teslas (Tesla), on the length in inches.

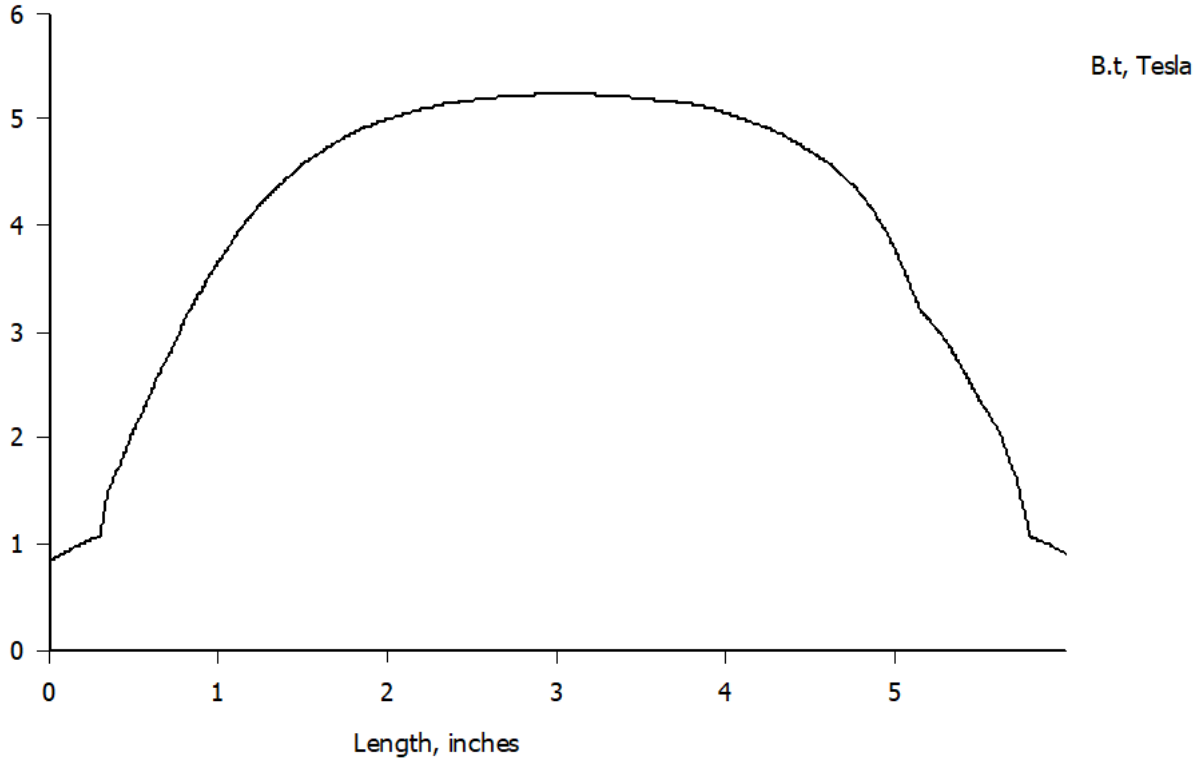

Figure 7.11 – Tangential flux density

Graph Description:

Initial section (from 0 to ~1 inch): The graph shows a gradual increase in tangential flux density from 1 to about 2 T, indicating a steady strengthening of the magnetic field.

Middle section (from ~1 to ~5 inches): There is a stable peak area with flux density values around 5 T, indicating a strong and steady tangential component of the magnetic field in this region.

Final section (from ~5 to 6 inches): The flux density gradually decreases back to around 1 T, suggesting a reduction in the tangential component of the flux.

The graph illustrates a smooth increase and decrease in tangential flux density along the length, reaching a maximum in the central region, which reflects the flux density distribution in this configuration.

The figure 7.12 displays the dependence of the magnetic field intensity |H|, measured in amperes per meter (Amp/m), on the length in inches.

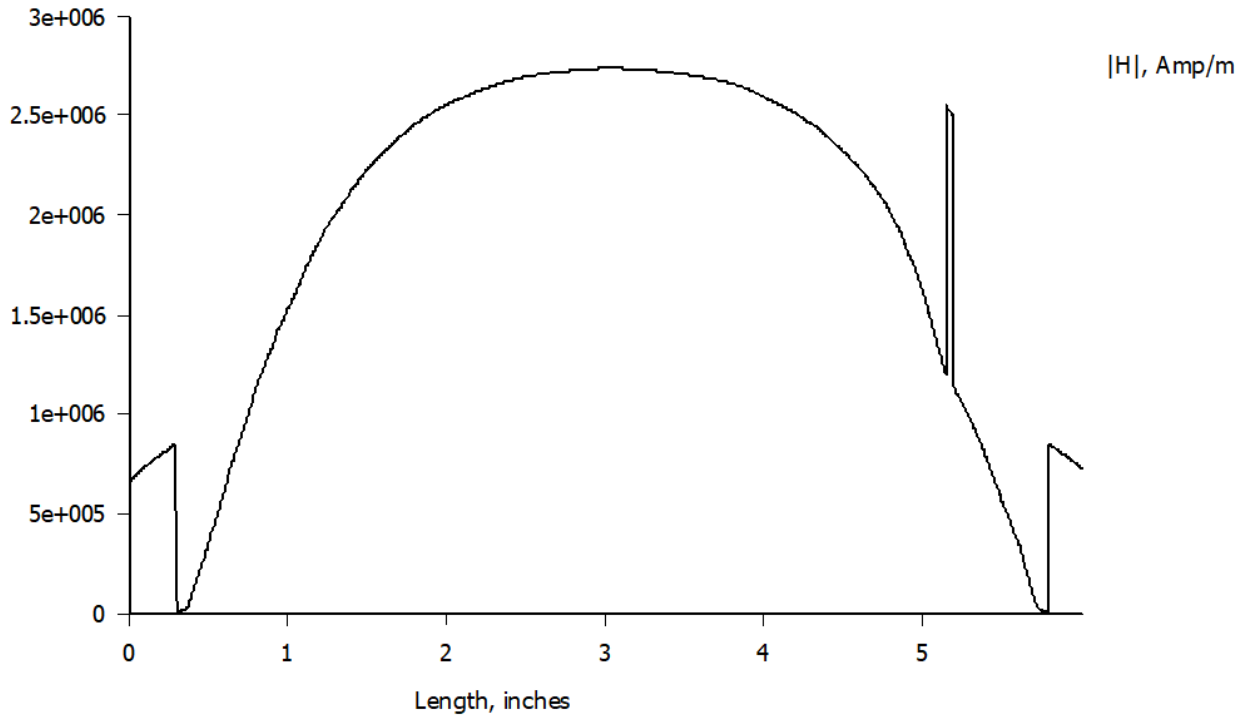

Figure 7.12 – Magnitude of field intensity

Graph Description:

Initial section (from 0 to ~1 inch): The graph shows a sharp increase in field intensity from zero to approximately 5e+5 A/m, indicating an initial rise in the magnetic field.

Middle section (from ~1 to ~5 inches): The magnetic field intensity reaches peak values around 2.5e+6 A/m and remains relatively stable at this level in the central region of the graph.

Final section (from ~5 to 6 inches): A steep drop in field intensity is observed, followed by several sharp peaks reaching up to 3e+6 A/m, and then a return to zero, indicating rapid fluctuations and a decline in field strength in this region.

The graph illustrates that the magnetic field intensity has a distinct maximum in the central part, accompanied by abrupt changes toward the edges.

The figure 7.13 illustrates the dependence of the normal component of magnetic field intensity Hn, measured in amperes per meter (A/m), on length in inches.

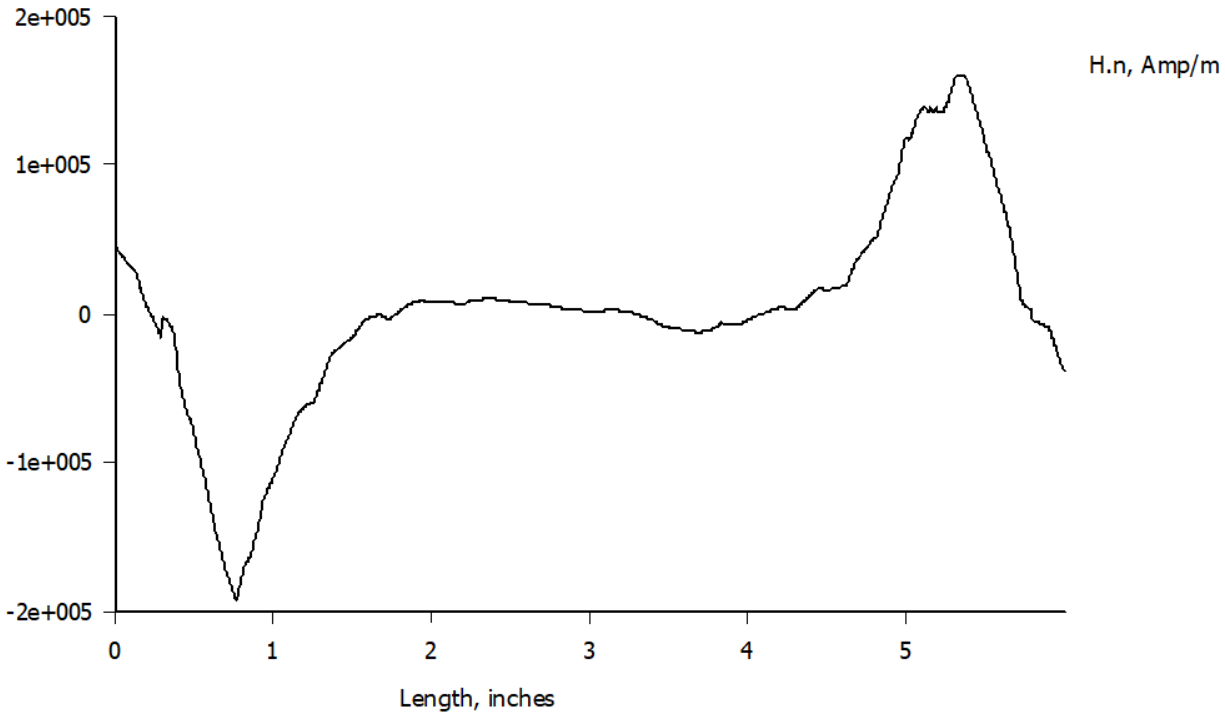

Figure 7.13 – Normal field intensity

Graph Description:

Initial section (from 0 to ~1 inch): There is a sharp decrease in Hn to around -2e+5 A/m, indicating an area with a strong reverse direction of the magnetic field.

Middle section (from ~1 to ~4 inches): The field intensity remains relatively stable with small fluctuations around zero, suggesting a weak field in this region.

Final section (from ~4 to ~6 inches): A sharp rise is observed, reaching a peak of around 1e+5 A/m, followed by a drop. This section shows significant changes in the magnetic field with distinct peaks, which may indicate inhomogeneities in the flux distribution.

The graph illustrates the variable normal magnetic field intensity along the length, with pronounced changes at the beginning and end.

The figure 7.13 shows the relationship between the tangential component of magnetic field intensity Ht, measured in amperes per meter (A/m), and length in inches.

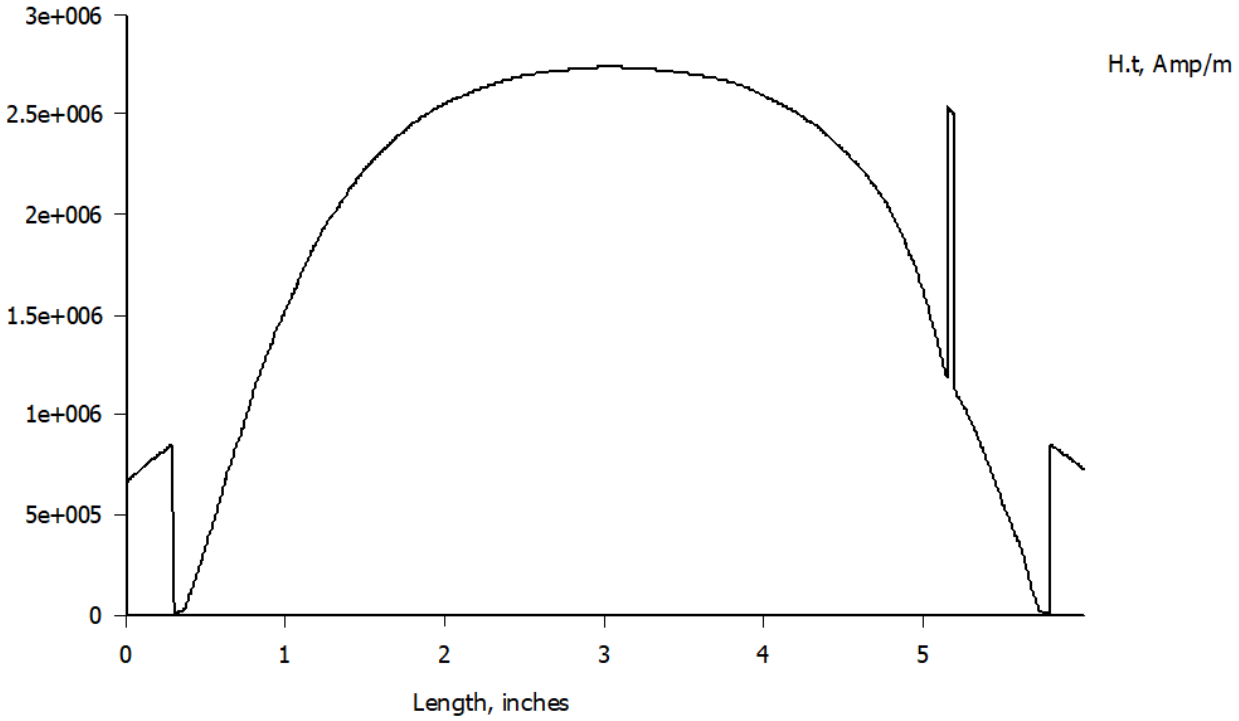

Figure 7.13 – Tangential field intensity

Graph Description:

Initial section (from 0 to ~1 inch): The graph shows a rapid increase in Ht from nearly zero to approximately 5e+5 A/m, indicating a strong initial rise in the magnetic field intensity.

Middle section (from ~1 to ~5 inches): The intensity stabilizes at a high level, with values reaching around 2.5e+6 A/m, showing a strong and steady tangential field in this central region.

Final section (from ~5 to 6 inches): There is a steep drop in intensity back to near zero, with a few sharp peaks exceeding 3e+6 A/m, suggesting fluctuations and a rapid decrease in the magnetic field at the edge of this region.

This graph illustrates a prominent peak in tangential field intensity at the center, with rapid changes near the boundaries.

CONCLUSION

Contactors are widely used in various industries to control electric motors, lighting systems, heating equipment, capacitor banks, thermal evaporators, and other electrical loads.

This master`s project involved designing an AC contactor with a rated current of 110 A (AC-1), a rated voltage of 380 V, and a control coil voltage of 220 V. The design was based on the magnetic starter model CEM 80.00 - 220 V, featuring a DC electromagnet. Additionally, several foreign models were reviewed for design insights.

In the course of this project, calculations were conducted for the current-carrying components. This included selecting and calculating output terminals, contact connections, switching mechanisms, contact wear and follow-through, and designing flexible couplings. Copper was chosen as the primary material for current-carrying elements, and silver coatings were applied to switching contacts to account for continuous operation. Thermal stability checks were performed on the output terminals, contact connections, and switching mechanisms.

The apparatus mechanism was then designed, resulting in the development of an opposing force characteristic curve. Preliminary calculations for the electromagnets were also conducted, determining magnetic circuit dimensions, the winding’s magnetizing force, and its geometrical dimensions.

For arc control, the free blowout method with two breaking points was selected, and the arc extinguishing process was verified under these conditions.

Additionally, calculations were conducted to determine the characteristics and required number of winding turns for stable operation of the apparatus.

Finally, an analysis of the electromagnet was performed using the FEMM software, which allowed for precise modeling of the electromagnet’s behavior and enabled parameter analysis with material selection, covering aspects such as magnetic field intensity, force distribution, and other various coefficients. The attractive force of the plate by the magnet was also calculated, amounting to 1332.54 N.

Schematics of the device and its primary components are included in the project.

LIST OF REFERENCES

1. Клименко Б. В. Електричні апарати. Електромеханічна апаратура комутації, керування та захисту. Загальний курс: навчальний посібник. — Харків: вид-во НТУ "ХПІ", 2012. — 320 с.
2. Braunovic M., Myshkin N. K., Konchits V. V. Electrical Contacts Fundamentals, Applications and Technology. — CRC Press, 2006. — 672 p.
3. Vasilega P. O. Electric drive of working machines: textbook. — Sumy State University, 2022. — 290 p.
4. Akimov L. V. Automated electric drive: elements, theory, control systems. 3000 questions for self-study and control of knowledge / L. V. Akimov, P. A. Kachanov, A. N. Cherenov. — Kharkiv: Publishing House "Textbook of NTUU "KhPI", 2011. — 532 p.
5. Klymenko B. V. Electric devices. Electromechanical switching, control and protection equipment. General course. Tutorial. — Kharkiv: NTU "KhPI" publishing house, 2012. — 320 p.
6. DSTU IEC 60898-1:2005. Auxiliary electrical equipment. Automatic circuit breakers for protection against overcurrents for household and similar applications.
7. Statsenko O. G. Guidelines for coursework and self-study in "Electrical Devices" for full-time students in the specialty 6.092204 - "Electromechanical Equipment for power generation". — Zaporizhzhia: ZNTU, 2010. — 42 p.
8. ГОСТ 434-78. Rectangular wire and copper bars for electrical purposes. Specifications.
9. URL: http://www.abb.com/product
10. URL: http://www.energy-group-ua.com
11. URL: https://leg.co.ua/knigi/ucheba/ustroystvo-es-ps-i-lep/Page-17.html
12. URL: https://www.eti.ua/produktsiya-ua/motor-contactor-cem-overload-relays-and-acessories/motor-contactor/004650201-cem80-00-110a-1000v-ac-37kw-0-0#accessories

13. URL: https://asmelectronica.com/product/kontaktor-kti-5115-115a-400v-as3-iek/
14. URL: https://www.skad.com.ua/kontaktor_af65-30-00-13/
15. URL: http://www.forca.ru/info/spravka/kontaktory-peremennogo-toka
16. Байда Е. І. Розрахунок електромагнітних та теплових полів за допомогою програми FEMM: навчально-методичний посібник. — Харків: НТУ «ХПІ», 2015. — 94 с.